ChemPhysMater 5 (2026) 391–404

Contents lists available at ScienceDirect

ChemPhysMater

journal homepage: https://www.keaipublishing.com/en/journals/chemphysmater/

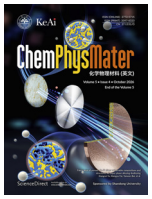

Review Article

Research progress of low-concentration electrolytes for sodium-based batteries

Kang Wang[a,b], Yongyao Feng[a], Jiajun Wang[a], Jiaxiang Zeng[a], Yuxin Guo[a], Jiayi Wang[a], Fangyuan Deng[a], Qi Peng[a], Feng Liu[a], Kuirong Deng[c], Kai Yang[d], Yilong Lin[a,*]

[a] College of Light Chemical Industry and Materials Engineering, Shunde Polytechnic University, Foshan 528333, China
[b] Guangzhou Great Power Energy & Technology Company Limited, Guangzhou 511483, China
[c] School of Applied Physics and Materials, Wuyi University, Jiangmen 529020, China
[d] College of Chemistry and Material Science, Shandong Agricultural University, Tai'an 271018, China

ARTICLE INFO

Keywords:
Sodium-based batteries
Nonaqueous electrolyte
Low cost
Low salt concentration
Interphasial chemistry

ABSTRACT

Sodium-based batteries (SBBs) have shown tremendous potential in large-scale energy storage applications due to their cost-effectiveness and natural abundance of sodium. Conventional views hold that low-concentration electrolytes (LCEs) struggle to achieve stable charge/discharge performance because of reduced ionic conductivity caused by low Na^+ concentrations. The research progress, performance regulation, and development prospects of low-concentration electrolytes have not been fully summarized. Low-concentration electrolytes (LCEs, typically <1 M) have presented significant potential for SBBs electrolytes owing to their advantages of cost-effectiveness, low viscosity and wide-temperature tolerance. However, they are confronted with critical challenges, specifically regarding low ionic conductivity and inadequate interfacial stability. This paper presents a systematic review of the recent advances in LCEs for SBBs, focusing on the regulatory mechanisms of solvent engineering, additive design, and salt systems and their concentrations on electrode/electrolyte interface (EEI) chemistry, and analyzes the synergistic effect between ion transport and interfacial stability under low-salt concentration. Finally, this paper analyzes the current challenges and prospects the future directions of multifunctional electrolyte design, providing new ideas for the low-cost and high-reliability development of SBBs.

Glossary of abbreviation

Abbreviation	Description
LIBs	Lithium ion batteries
SIBs	Sodium ion batteries
SMBs	Sodium metal batteries
SBBs	Sodium-based batteries
LCEs	Low-concentration electrolytes
EEI	Electrode/electrolyte interface
LUMO	The lowest unoccupied molecular orbital
HOMO	The highest occupied molecular orbital
SEI	Solid electrolyte interphase
CEI	Cathode electrolyte interphase
SSIP	Solvent-separated ion pair
CIPs	Contact ion pairs
AGGs	Cation-anion aggregates
HCE	High-concentration electrolyte
LHCE	Localized high-concentration electrolyte
DMC	Dimethyl carbonate
DEC	Diethyl carbonate
EMC	Ethyl methyl carbonate
EC	Ethylene carbonate
PC	Propylene carbonate
P/N ratio	Positive/negative ratio
GITT	Galvanostatic Intermittent Titration Technique
BSTFA	N, O-bis(trimethylsilyl) trifluoroacetamide
TTE	1,1,2,2-Tetra-fluoroethyl-2,2,3,3-tetrafluoropropyl ether
TMP	Trimethyl phosphate
TEP	Triethyl phosphate
HC	Hard carbon
PW	Prussian white
NaBOB	Sodium bis(oxalato)borate
LiBOB	Lithium bis(oxalato)borate
PFPN	Ethoxy(pentafluoro) cyclotriphosphazene
DME	Dimethoxy ethane
DEGDME	Bis(2-methoxy ethyl)ether
DOL	1,3-dioxolane
FEC	Fluoroethylene carbonate
DFEC	*Trans*-difluoroetyhene carbonate

(*continued on next page*)

(*continued on next page*)

* Corresponding author.
E-mail address: 23084@sdpt.edu.cn (Y. Lin).

https://doi.org/10.1016/j.chphma.2026.03.008
Received 13 January 2026; Received in revised form 10 March 2026; Accepted 31 March 2026
Available online 4 April 2026
2772-5715/© 2026 The Authors. Publishing Services by Elsevier B.V. on behalf of KeAi Communications Co. Ltd. This is an open access article under the CC BY-NC-ND license (http://creativecommons.org/licenses/by-nc-nd/4.0/)

TMSB	tris(trimethylsilyl)borate
NaDFOB	Sodium oxalyldifluoroborate
VC	Vinylene carbonate
ETFA	1 wt% 2,2,2-trifluoroethyl acetate
NaOTf	sodium trifluoromethanesulfonate
NaTFSI	Sodium bis(trifluoromethanesulfonyl)imide
NaFSI	Sodium bis(fluorosulfonyl)imide
NaTDI	4,5-dicyano-2-(trifluoromethyl)imidazolate
DWIE	Dual-weak-interaction electrolyte
DBE	Dibutyl ether
Melm	1-methylimidazole
$PhCF_3$	Trifluorotoluene
CE	Coulombic efficiency
THF	Tetrahydrofuran
HF	Hydrofluoric acid
CN	Coordination number
NVPF	$Na_3V_2(PO_4)_2F_3$
NVP	$Na_3V_2(PO_4)_3$
XPS	X-ray photoelectron spectroscopy
TOF-SIMS	Time of flight secondary ion mass spectrometry
EIS	Electrochemical impedance spectroscopy
LSV	Linear sweep voltammetry
TEM	Transmission electron microscopy

1. Introduction

Sodium-based batteries (SBBs), including sodium-ion batteries (SIBs) and sodium metal batteries (SMBs), as a prospective energy storage technology with significant economic benefits, exhibit broad application prospects in applications such as grid-scale energy storage and electric vehicles. Compared with lithium-ion batteries (LIBs), sodium has an abundance of up to 2.75% in the earth's crust and is inexpensive, endowing SBBs with inherent cost advantages in large-scale energy storage scenarios [1,2]. However, the ionic radius of sodium ions (Na^+, 1.02 Å) is larger than that of lithium ions (Li^+, 0.76 Å), leading to slower diffusion kinetics in electrode materials and poor stability of the electrolyte interface. These two major challenges restrict the practical application of SBBs [3,4]. As the medium for ion transport in batteries, the electrolyte properties influence the cycle life, rate performance, and operating temperature range of the battery. Therefore, the optimization of the electrolyte system has become one of the key directions to break through the performance bottleneck of SBBs.

In traditional electrochemical energy storage systems, the design of electrolyte concentrations has often followed the "1 M concentration paradigm", which assumes that a salt concentration of approximately 1 mol/L represents the optimal choice for balancing ionic conductivity and interfacial stability. This understanding originates from early research on non-aqueous electrolyte systems, which proposed that higher salt concentrations can provide more ionic carriers, thereby enhancing ionic conductivity [5]. However, with the in-depth investigation of electrolyte-electrode interfacial chemistry, researchers have found that concentration regulation not only affects the physicochemical properties of the bulk electrolyte but also exerts a significant influence on the composition and structure of the EEI, thereby determining the long-term stability of the battery [6].

In the field of lithium-ion batteries, significant progress has been made in the research of high-concentration electrolytes (HCEs) and localized high-concentration electrolytes (LHCEs). Compared to the 1 M concentration, in HCEs and LHCEs, there are nearly no free solvent molecules, with more anions participating in the solvation of Li^+. HCEs and LHCEs enhance the interaction between salts and solvents, forming a solvation structure dominated by contact ion pairs (CIPs) and aggregates (AGGs) [7]. This promotes anions to participate in the formation of interfacial films, thus constructing a stable solid electrolyte interphase (SEI) film with rich inorganic components (such as LiF). However, HCEs necessitate a large amount of salts, which not only drives up material costs substantially but also complicates the preparation procedure [8]. For example, in a 1 M $LiPF_6$ electrolyte, the cost of lithium salts accounts for >60% of the total. When the concentration increases to 3 M, the salt dosage triples, making the cost problem more prominent. Additionally, the heightened viscosity of HCEs can impair electrolyte wettability on the separator and electrodes, thereby deteriorating battery performance, especially under low-temperature conditions. To address the issues of HCEs, researchers have proposed a novel electrolyte system, LHCEs, which can effectively mitigate the aforementioned issues by incorporating inert diluents into HCEs. The introduction of diluents effectively lowers the total salt concentration in LHCEs, while retaining the local coordination environment of high-concentration salt-solvent clusters inherent to HCEs, enabling LHCEs to exhibit excellent wettability and high ionic conductivity [9]. While current LHCE formulations typically incorporate highly fluorinated ethers, fluorinated carbonates, fluorobenzene, and fluorinated alkanes as diluents, these fluorinated solvents present notable drawbacks compared to conventional carbonate- or ether-based electrolyte solvents [10]. Specifically, they are characterized by higher toxicity, elevated costs, and increased environmental hazards—including significant ozone layer depletion potential and substantial ecological damage [11]. The environmental repercussions and toxicity concerns mandate the adoption of safer handling protocols or the development of alternative strategies to enable more sustainable utilization of these solvents.

In contrast, LCEs demonstrate distinct advantages over conventional or high-concentration systems, including enhanced charge transfer kinetics, improved wettability, and lower viscosity (Figs. 1(a)(b)) [12,13]. Notably, considering that salts are approximately ten times more expensive than solvents, the manufacturing costs of LCEs are reduced owing to their decreased consumption of salts. Different from lithium-ion batteries, the electrolyte concentration regulation in NIBs presents a unique research pathway. Due to the smaller Stokes radius of Na^+ compared to Li^+ and its significantly lower desolvation energy (~0.5 eV vs. ~0.7 eV for Li^+), Na^+ maintains fast ionic migration rates [14]. Na^+ possesses higher ionic conductivity than Li^+ in most nonaqueous electrolytes. This characteristic enables SBBs to maintain sufficient ionic conductivity even in dilute solutions. Given that Na^+ exhibits superior ionic conductivity and reduced desolvation energy compared to Li^+ in liquid electrolytes, and when coupled with the low viscosity and excellent wettability advantages of LCEs, SBBs are anticipated to demonstrate enhanced rate capability and low-temperature performance relative to lithium batteries [15]. Therefore, the research on low-concentration electrolytes can offer new directions and insights for the studies of SIBs and SMBs. For example, investigations into the solvation structure, interfacial chemistry, and ion transport mechanisms of low-concentration electrolytes help deepen the understanding of SIB/SMB working principles, providing theoretical support for developing more advanced SBBs. Furthermore, studies on low-concentration electrolytes have proposed new strategies for the stable operation of low-cost SBBs, as their large-scale deployment in grid energy storage systems demands economically viable solutions.

In recent years, significant breakthroughs have been achieved in the research of LCEs for SBBs (Fig. 1(c)). Current studies focus on reducing salt concentration while preserving the unique anion-induced solvation structure and efficient cation transport. The co-solvents design and the solvent-solvent interaction regulation, as well as the adoption of dual-salt systems or combinations of multiple sodium salts with different solvated anions, has become important approaches to regulate the solvation structure and interfacial chemistry of SBBs, and further serve as key breakthrough points for the development of high-performance and low-cost functional electrolytes. In general, studies on the correlation between salt concentration and solvation structure provide a feasible solution for achieving targeted interfacial chemistry (structure) design in sodium secondary batteries. For specific application scenarios such as low impedance, high voltage resistance, and long cycling, engineering strategies involving the special design and combination of functional additives to address the critical issue of unstable electrode-electrolyte

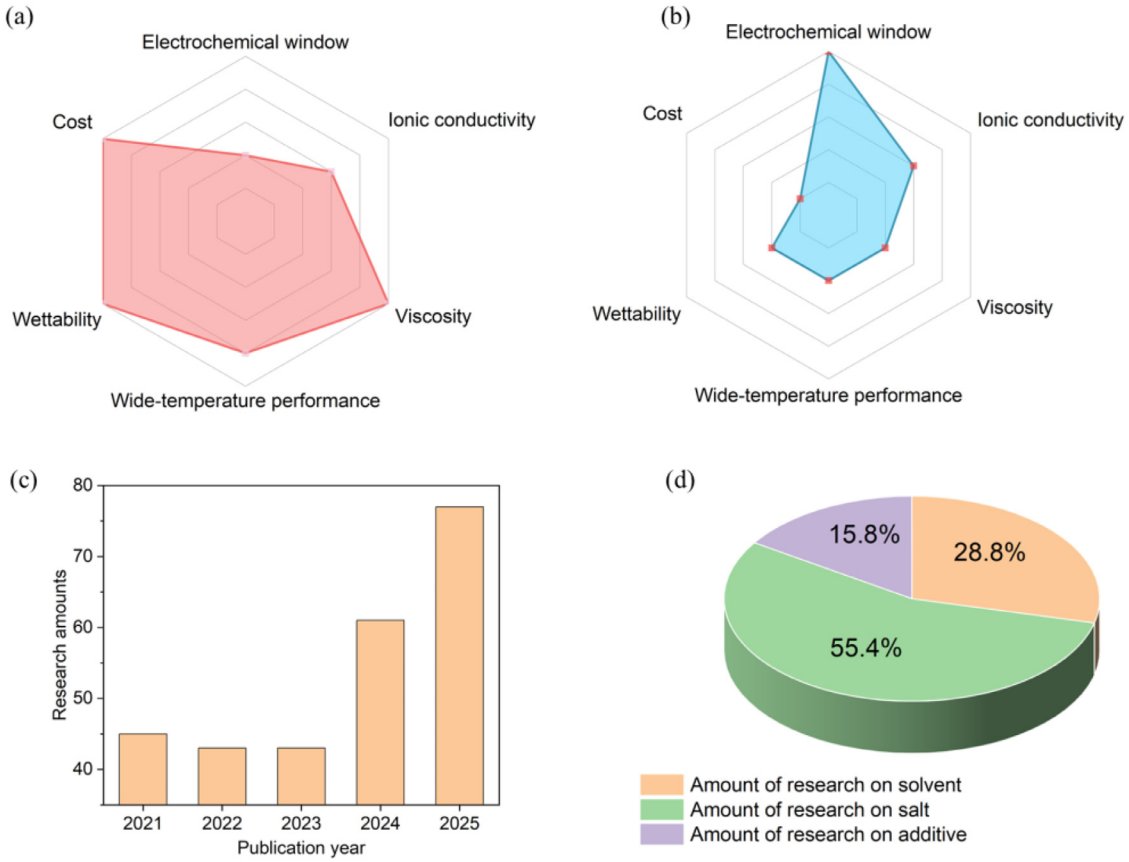

Fig. 1. The performance comparisons of LCEs (a) and HCEs (b). (c) Annual publication count regarding ether-based electrolytes in sodium-based batteries from 2021 to 30th December 2025. Web of Science search keywords included "low concentration", "electrolyte" and "sodium battery". (d) Proportion of research on solvent, salt and additive (from 2021 to 30th December 2025).

interfaces in low-concentration electrolytes are crucial for improving battery performance (Fig. 1(d)).

Meanwhile, the application of LCEs in SBBs faces three major challenges including solvent structure, ion transport, and interface evolution (Fig. 2). 1) The low ion-solvent ratio in LCEs leads to a solvation structure dominated by solvent-separated ion pairs (SSIPs). Excessive free solvent molecules weaken cation-anion interactions, resulting in insufficient anion participation in solvation sheaths. 2) The low salt concentration reduces the number of ionic carriers, leading to relatively low intrinsic ionic conductivity; beside, the weak solvation environment and uneven solvation sheath distribution result in inconsistent ion migration paths, increasing concentration polarization during high-rate or low-temperature operation. 3) Free solvent molecules in LCEs are prone to preferential decomposition on electrode surfaces, forming organic-rich, loose, and soluble SEI/CEI layers. These layers lack inorganic components with high mechanical strength and ion conductivity, leading to continuous electrolyte consumption, interface thickening, and increased ion transport resistance.

This review focuses on the basic design principles, solvation structure regulation strategies, and effective methods for optimizing interfacial chemistry, while summarizing the advanced characterization techniques currently applied in LCE research. The paper systematically synthesizes the action mechanisms of solvent engineering, additive design, and salt system optimization in enhancing the performance of low-concentration SBBs, and outlines the future development directions and challenges in this field. This review aims to serve as a comprehensive reference for research on low-concentration SBBs and promote their practical application process in the energy storage field.

2. Solvent engineering

2.1. Carbonate solvents

Carbonate-based solvents have long been the dominant choice for electrolytes in alkali metal ion batteries [16]. Undoubtedly, the most cost-effective strategy involves the direct modulation of carbonate electrolyte compositions. Carbonate-based solvents, including diethyl carbonate (DEC), dimethyl carbonate (DMC), ethyl methyl carbonate (EMC), ethylene carbonate (EC), and propylene carbonate (PC), exhibit excellent electrochemical stability and ion transport capability. As crucial parameters, the viscosity and dielectric constant of solvents both exert a significant influence on the ionic conductivity of electrolytes. However, carbonate solvents possess relatively low oxidative stability and high reactivity with sodium metal anodes [17]. In carbonate-based LCEs, electrolyte instability becomes more prominent due to the presence of a large amount of free solvent [18]. Thus, an ideal strategy for realizing its application involves the construction of an interfacial film characterized by high ionic conductivity and low electronic conductivity. Studies have demonstrated that anion-dominated solvation structures play a critical role in the film-forming process of HCEs and LHCEs. Therefore, for low-concentration electrolytes in sodium-ion batteries, solvent engineering, such as the adoption of non-solvating co-solvents, can be employed to enhance electrochemical performance (Table 1).

EC exhibits a strong ability to dissociate lithium salts due to its high dielectric constant (89.78) and can form a relatively stable passivation layer through reduction on the surface of carbon-based anodes. However, EC has a relatively high melting point (36.4 °C), which impairs

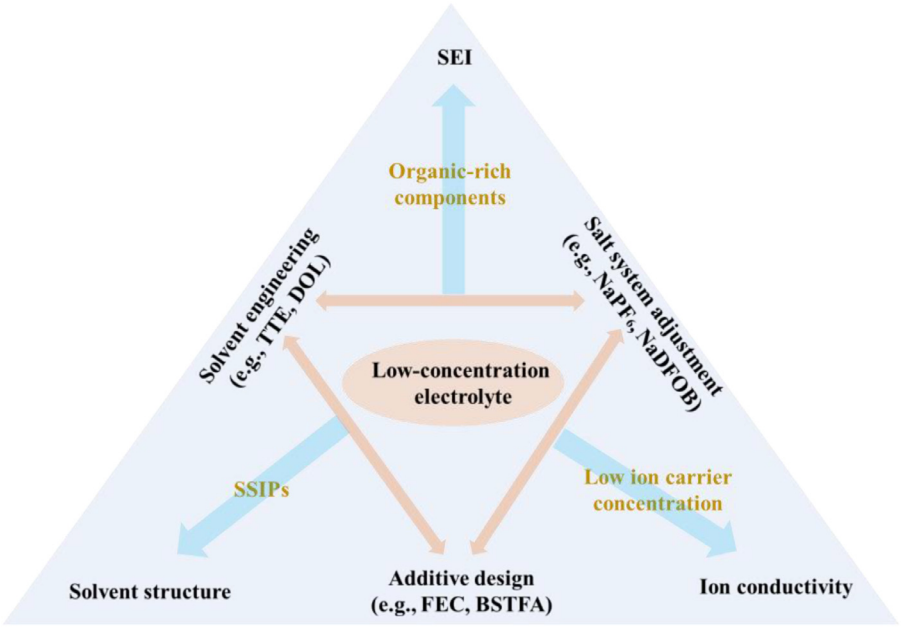

Fig. 2. Relations between LCEs and SEI, solvent structure and ion conductivity.

Table 1
Summary of the Na-based batteries using carbonate-based electrolyte.

Electrolyte formulation	Cell system	Capacity (mAh g^{-1}) or Capacity retention/Cycle Number/C rate	Cycle voltage range/Operating temperature	Ref.
0.1 M $NaClO_4$ in PC with 2%FEC	Hard carbon/ $Na_{0.90}Cu_{0.22}Fe_{0.30}Mn_{0.48}O_2$	80% after 200 cycles/1 C	2–4 V/25 °C	[19]
0.3 M $NaPF_6$ in EC/PC	Disordered carbon/ $Na[Cu_{1/9}Ni_{2/9}Fe_{1/3}Mn_{1/3}]O_2$	~95% after 50 cycles/0.3 C	1.0–4.0 V/25 °C	[20]
0.3 M $NaPF_6$ in EC/PC with 2 wt% N, O-bis(trimethylsilyl)trifluoroacetamide	$Na/Na_3V_2(PO_4)_3$	92.63% after 1955 cycles /2 C	2–4 V/40 °C	[21]
0.3 M $NaClO_4$ in EC/PC with 5%FEC	Hard carbon/ $Na_3V_2(PO_4)_2F_3$	93.4% after 1000 cycles/1 C	2.5–4.5V/−25 °C	[22]
0.3 M $NaPF_6$ in PC/EMC with 1% 2,2,2-trifluoroethyl acetate	HC/FeNi-MnHCF	92.1% after 1120 cycles/1 C	1.5–3.7 V/−20 °C	[23]
0.6 M $NaPF_6$ in EC/FEC	$Na/Na_{0.75}Ni_{0.34}Mn_{0.66}O_2$	85.4% after 160 cycles/0.5 C	2.4–4.15 V/−40 °C	[24]
0.5 M $NaClO_4$ in EC/PC/DEC with 5 wt% FEC	$Na/Na_4Fe_3(PO_4)_2(P_2O_7)$	90.5 mAh g^{-1}/300 cycles/0.5 C	1.7–4.2 V/30 °C	[25]
0.3 M $NaPF_6$ in PC/FEC/TTE	Na/ $Na_4Co_3(PO_4)_2P_2O_7$	94.25% after 150 cycles/1 C	3–4.7 V/25 °C	[26]
0.3 M $NaPF_6$ in PC/FEC/TTE	$Na||FePO_4$	94.8% after 350 cycles/0.5 C (charge)/1 C (discharge)	1.5–4 V/25 °C	[27]

the low-temperature performance of batteries. PC, with advantages of low cost and a wide temperature window, is considered an organic solvent that can be used alone in sodium-ion electrolytes. In lithium-ion batteries, PC undergoes continuous reductive decomposition at potentials prior to lithium intercalation (~0.7 V), ultimately leading to the collapse of the graphite structure. In contrast, the use of PC in hard carbon anodes for sodium-ion batteries is relatively stable. Zhang et al. [19] tested 5 electrolytes (1 M $NaClO_4$ in EC/PC; 0.1 M $NaClO_4$ in PC; 1 M $NaPF_6$ in EC/PC; 0.7 M $NaPF_6$ in PC/EMC; 0.1 M $NaPF_6$ in EC/DMC) for $Na_{0.90}Cu_{0.22}Fe_{0.30}Mn_{0.48}O_2$ /HC SIBs and the optimal was 0.1 M $NaClO_4$ in 100% PC. The electrolyte balanced ionic conductivity and interfacial stability, achieving 80.2 mAh g^{-1} initial capacity (0.1 C) and 84.3% retention after 200 cycles (1 C) at P/N ratio 0.9, while GITT tests revealed low overpotential-driven irreversible heat. Although the adoption of a low sodium salt concentration can reduce viscosity, the issue of limited ion mobility and poor film-forming ability still persists when using PC as a single solvent. Thus, blending two or three distinct solvents to optimize the electrochemical performance of electrolytes is a commonly adopted strategy in relevant research and applications.

Li et al. [20] first proposed an ultralow-concentration electrolyte (0.3 M $NaPF_6$ in EC/PC), leveraging the smaller Stokes radius of Na^+ and lower desolvation energy to maintain sufficient ionic mobility. This electrolyte exhibited low viscosity (≈3 cP vs. ≈10 cP of 1 M electrolyte), excellent wettability on high-loading electrodes, and an organic-dominated SEI/CEI, enabling stable cycling across −30 to 55 °C and reducing salt cost by 70% (Figs. 3(a)(b)). Building on this, N, O-bis(trimethylsilyl) trifluoroacetamide (BSTFA) was introduced as an additive to 0.3 M $NaPF_6$/EC-PC, which scavenged HF/H_2O, inhibited $NaPF_6$ hydrolysis, and formed a NaF-rich organic SEI/CEI. The modified electrolyte enhanced $Na||Na_3V_2(PO_4)_3$ cell performance, achieving 92.63% capacity retention after 1955 cycles at 2 C and 105 mAh g^{-1} at 40 C, solving LCEs' poor compatibility with Na metal anodes (Figs. 3(c)–(f)) [21]. The cells with a binary PC/EMC solvent and 0.5 M $NaPF_6$ retained 92.1% capacity after 1120 cycles at 1 C/−20 °C and tolerated overcharge/overdischarge, demonstrating LCEs' potential for low-temperature large-scale storage [23]. Huang et al. [24] developed a 0.6 M $NaPF_6$-EMC/FEC electrolyte for SMBs. Its weakly anion-driven solvation boosted Na^+ conductivity and reduced desolvation barriers, forming a NaF-rich SEI (Figs. 3(g)(h)). Paired with P2-type $Na_{0.75}Ni_{0.34}Mn_{0.66}O_2$, SMBs retained 91.5% capacity after 600 cycles at −20 °C and 85.4% at −40 °C; a high-loading pouch cell delivered 227.4 Wh kg^{-1}.

In ternary solvent systems, the incorporation of a weakly solvating co-solvent enables the construction of an electrolyte featuring anion-rich clusters and fast Na^+ transport kinetics. This electrolyte is well-suited for SBBs that require fast charging capabilities and high energy den-

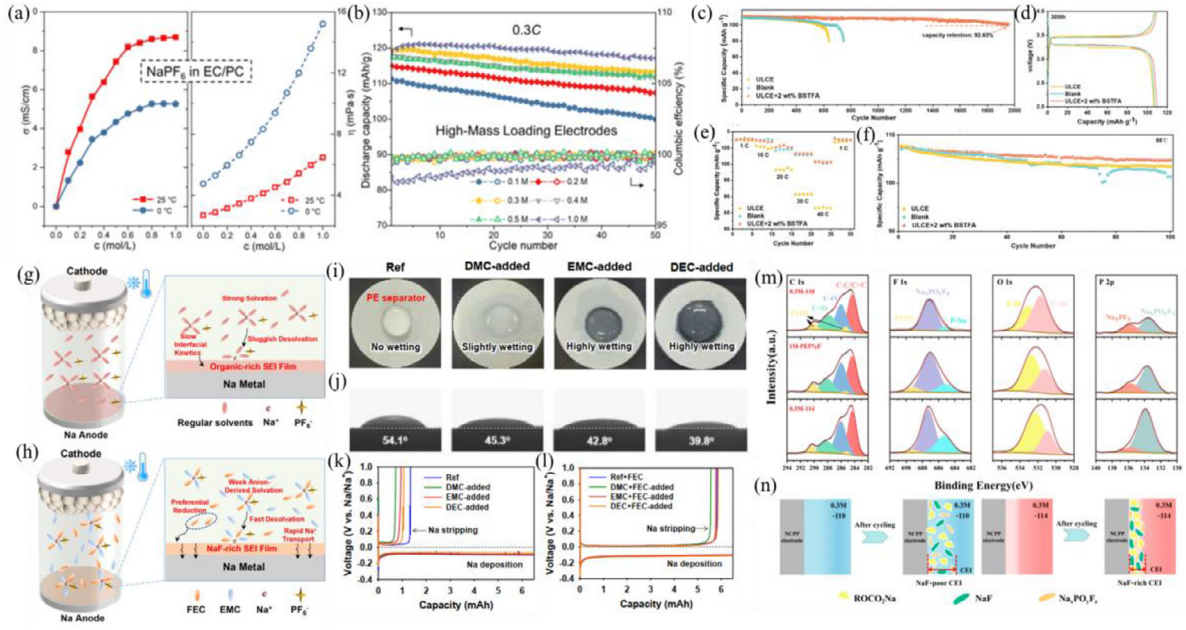

Fig. 3. (a) Variation of ionic conductivity and viscosity with concentration for $NaPF_6$ in EC/PC at 25 and 0 °C. (b) Cycling behavior of NIBs using electrolytes with different concentrations at 0.3 C (30 mA g^{-1}) and 25 °C. Reproduced with permission [20]. Copyright 2020, American Chemical Society. (c)–(f) Electrochemical performance of Na/NVP cells with different electrolytes: (c) cycling stability, (d) charge−discharge curves at the 300th cycle, (e) rate capability, (f) cycling performance at 55 °C. Reproduced with permission [21]. Copyright 2021, Elsevier. Schematic diagrams illustrating the operational mechanisms of (g) conventional electrolytes and (h) 0.6 M EF for LT-SMBs. Reproduced with permission [23]. Copyright 2025, Elsevier. (i) Digital photographs of various electrolytes adsorbed on PE separators in a dry room (dew point: −56 °C). (j) Contact angle measurements of the electrolytes on PE separators. Voltage profiles of Na/SS cells (k) without and (l) with 5 wt% FEC, depicting Na deposition and stripping at a C/10 rate. Reproduced with permission [24]. Copyright 2016, Elsevier. (m) XPS spectra (C 1s, O 1s, F 1s, P 2p) of NCPP cathodes after 153 cycles in different electrolytes. (n) Schematic illustration of the CEI formation mechanism in the different electrolytes. Reproduced with permission [26]. Copyright 2023, American Chemical Society.

sity. Lee et al. [25] explored linear carbonate-containing LCEs (0.5 M $NaClO_4$ in EC/PC/DEC) with FEC additive. The electrolyte formed a protective film on Na metal and $Na_4Fe_3(PO_4)_2(P_2O_7)$ cathode, suppressing linear carbonate decomposition, improving PE separator wettability, and enabling 97.5% capacity retention after 300 cycles at 0.5 C, overcoming linear carbonates' high reactivity (Figs. 3(i)–(l)). 1,1,2,2-Tetrafluoroethyl-2,2,3,3-tetrafluoropropyl ether (TTE) is widely utilized as a diluent solvent in lithium-ion batteries. This is attributed to its favorable characteristics, including an ultra-low freezing point of −115 °C, enhanced wettability toward electrode/separator components, dependable thermal stability at elevated temperatures, and inherent non-flammable nature [28]. In 0.3 M $NaPF_6$-PC/FEC, TTE as co-solvent was designed for high-voltage SIBs. TTE adjusted Na^+ solvation, enhancing oxidation stability to 5.0 V and forming a thin NaF-rich CEI (Figs. 3(m)(n)). The cells based on low-carbon $Na_4Co_3(PO_4)_2P_2O_7$ achieved 95.7 mAh g^{-1} initial capacity and 94.25% retention after 150 cycles at 4.7 V, and exhibiting the non-flammability [26]. In 0.3 M $NaPF_6$-PC/FEC/TTE electrolyte for wide-temperature SMBs, due to the low viscosity and fast Na^+ diffusion, the cells retained 92.8% capacity at 25 °C, 98.5% at 55 °C, and stable cycling at −20 °C, outperforming 1 M electrolytes via tailored solvation and SEI [27].

2.2. Non-carbonate solvents

While carbonate-based solvents lay the foundation for LCEs' basic ion transport and interfacial stability through solvation structure optimization, they face substantial barriers to widespread application in SBBs. A key issue lies in their tendency to form a SEI layer that is both soluble and continuously thickens over cycling, while they also exhibit poor stability when in contact with electrodes [29]. Non-carbonate solvents address key limitations of carbonates in sodium-ion and sodium metal batteries, such as flammability, interface instability, and poor low-temperature performance. Phosphates including trimethyl phosphate (TMP) and triethyl phosphate (TEP) have been adopted as flame-retardant solvents in low-concentration sodium batteries. This is attributed to their excellent flame retardance, a property that has also led to their widespread application in the fire-fighting industry [30]. 0.5 M NaBOB/TMP electrolyte decomposes to form a carbonate-rich SEI on hard carbon (HC) anodes, stabilizing the HC-TMP interface by inhibiting solvent co-intercalation. This SEI enables 84.3% capacity retention over 200 cycles in HC//Prussian white (PW) full cells. The room-temperature ionic conductivity of the electrolyte reaches 5 mS cm^{-1}, which is comparable to that of standard electrolytes utilizing $NaPF_6$ and organic carbonates (Fig. 4(a)). With a first-cycle Coulombic efficiency (CE) exceeding 80%, the proposed electrolyte demonstrates a CE of roughly 97% starting from the second cycle in HC/Prussian white full cells. After the flammability tests, TMP did not ignite for any concentration of NaBOB (Fig. 4(b)) [31]. The same HC/Prussian white battery system using non-toxic 0.38 M NaBOB-TEP electrolyte achieved a discharge capacity of 107 ± 4 mAh g^{-1} at the 1005th cycle (Fig. 4(c)). MD simulations demonstrated that ~35% of Na^+ form CIPs with BOB^- through coordination with the anion's double-bonded oxygens (Fig. 4(d)), which is consistent with the moderate ion-pairing degree (Fig. 4(f)). For fully solvated Na^+, they are coordinated by ~5 TEP molecules via P=O double-bonded oxygens, adopting a square pyramidal geometry (Figs. 4(e)(g)). This unique solvation structure with moderate ion-pairing and stable Na^+-TEP coordination, ensures sufficient ionic conductivity (>1 mS cm^{-1} at −30 °C) and effective SEI formation [32]. Weakly polar fluorinated ethoxy(pentafluoro)cyclotriphosphazene (PFPN) as a co-solvent was used to stabilize PC solvent in the low-concentration salt electrolyte. The intermolecular interaction between PC and PFPN improves the energy barrier of oxidation of PC and decreases the activity of PC (Fig. 4(h)), and leads to the reconstruction of cation/anion solvation structures (Fig. 4(i)). PFPN is distributed in the second solvation shell of Na^+, provides space for solvated Na^+ migration, accelerating the desolvation kinetics of Na^+ and enhancing the

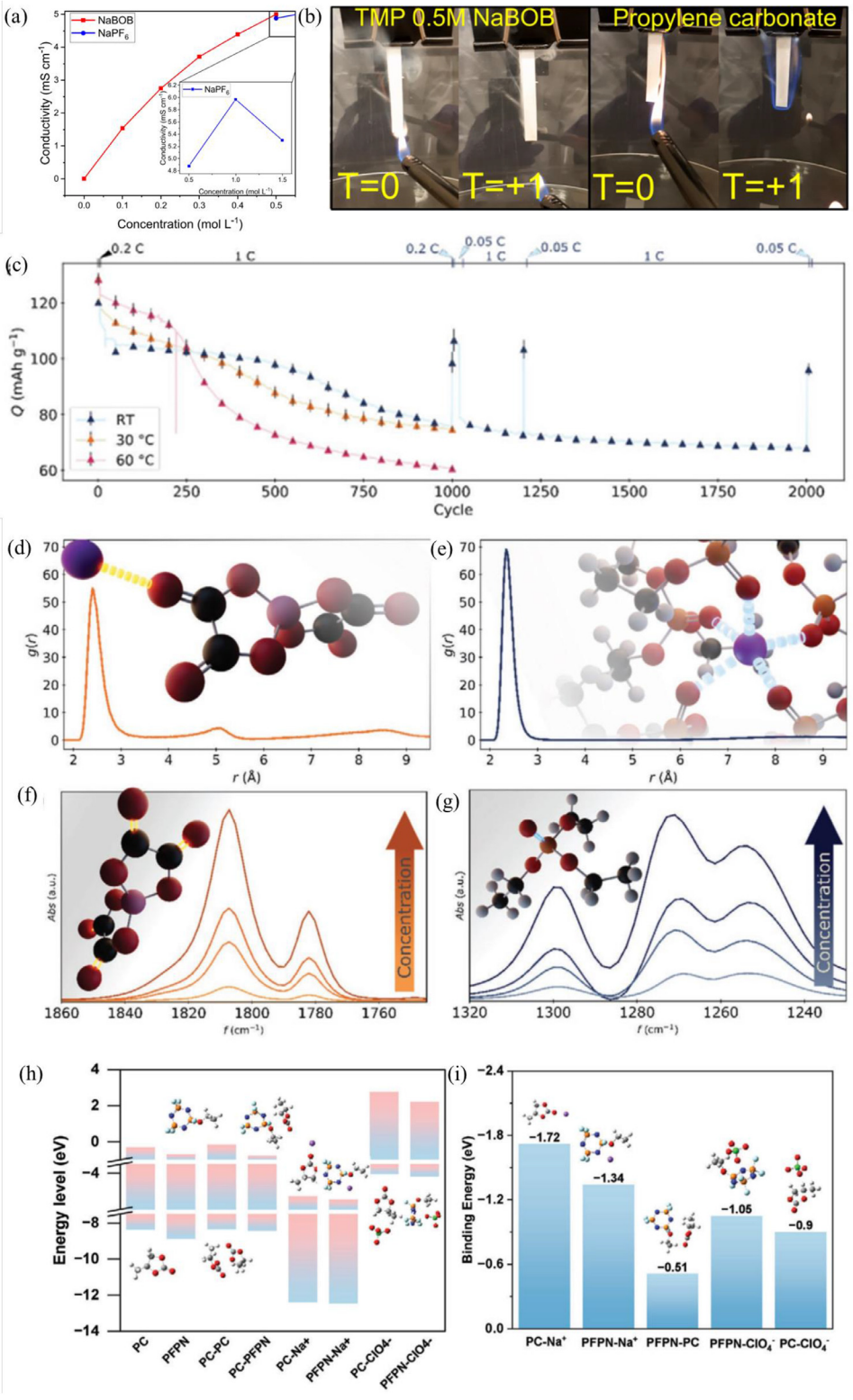

Fig. 4. (a) Ionic conductivity of NaBOB and $NaPF_6$ solutions in TMP. (b) Flammability tests of 0.5 M NaBOB in TMP (left) and PC (right). Reproduced with permission [31]. Copyright 2020, American Chemical Society. (c) Average discharge capacity at 30, 60 °C, and room temperature. The radial distribution function for (d) paired sodium-ions and the BOB-anion's coordinating oxygen; (e) free sodium-ions and the doublebonded oxygen on TEP. The differential IR absorption with increasing salt concentration, for the double bonded oxygens on (f) the BOB-anion and (g) the TEP molecule. Reproduced with permission [32]. Copyright 2021, Wiley-VCH. HOMO and LUMO values (h) and the binding energy (i) of different components. Reproduced with permission [33]. Copyright 2024, Wiley-VCH.

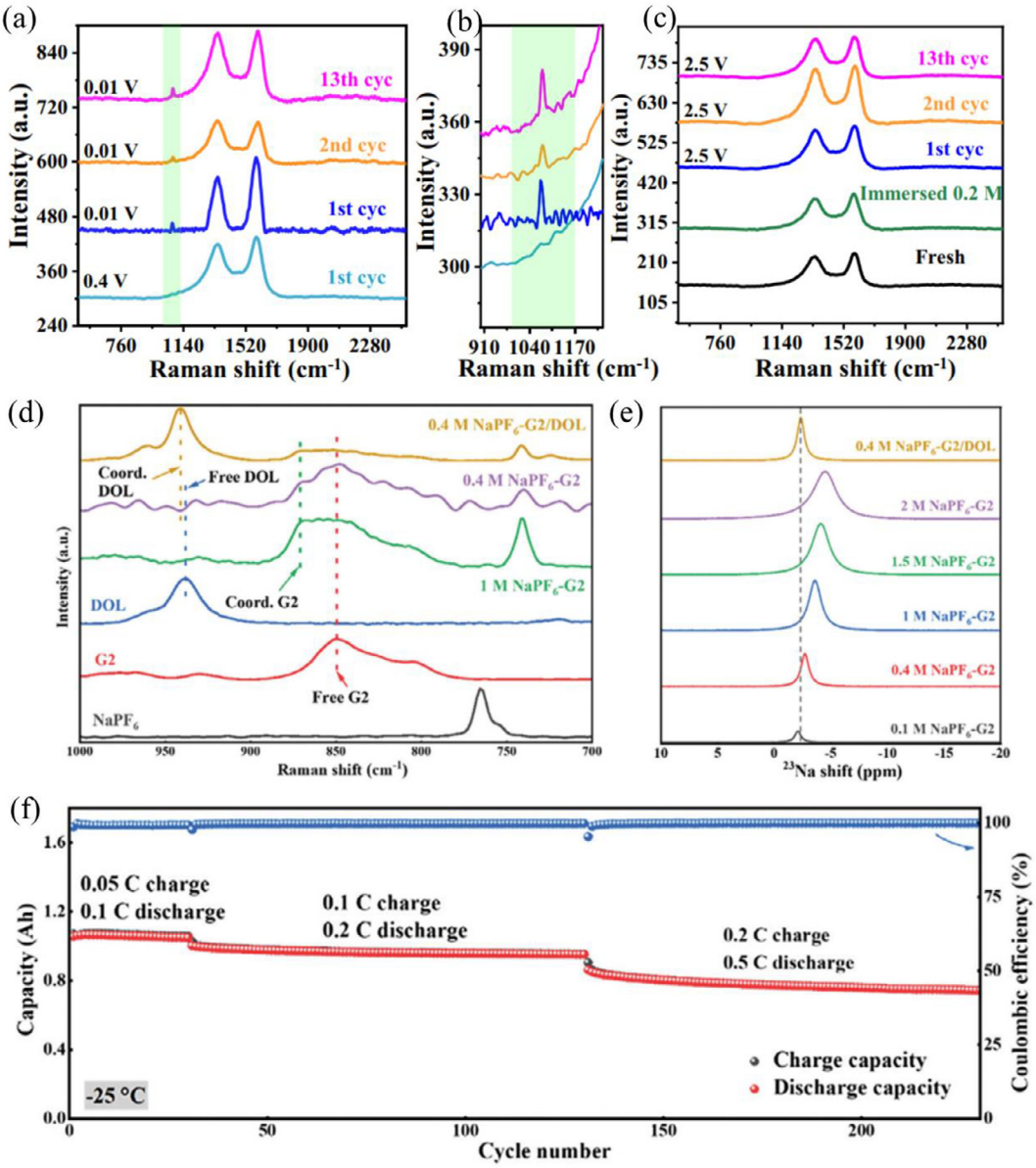

Fig. 5. Raman spectra of s-HC electrodes cycling with 0.2 M diglyme-based electrolyte, (a) charging to 0.4 V and 0.01 V and (b) the corresponding enlarge profiles; (c) discharging to 2.5 V. Reproduced with permission [34]. Copyright 2023, Elsevier. Raman spectra (d) and ^{23}Na NMR spectra (e) of various electrolytes and components; (f) cyclability of as-fabricated pouch cell at low temperature. Reproduced with permission [39]. Copyright 2024, Wiley-VCH.

antioxidant stability of the electrolyte. As a result, the ionic conductivity of designed electrolyte increases to 6.12 mS cm^{-1} and the oxidation stability is extended to 4.84 V [33].

Ether-based electrolytes have emerged prominently in the field of secondary batteries, owing to their unique physicochemical properties. In recent years, the application of ether solvents in low-concentration sodium-based batteries has garnered extensive attention. The stable solvation structure not only facilitates reversible solvent co-intercalation at the electrode/electrolyte interface but also promotes the generation of a thin and robust SEI. However, the mechanism underlying the performance enhancement of HC anodes by ether-based electrolytes remains controversial, with the core debate focusing on whether an SEI layer is formed during cycling. Zeng et al. [34] adjusted the $NaPF_6$ concentration to 0.2 M in DME-based electrolytes to accommodate the dual low voltage (<0.1 V) storage mechanisms in HC, including SEI-free Na^+-diglyme co-interactionand SEI-assisted desolvated Na^+ insertion (Figs. 5(a)–(c)). Benefiting from the discontinuous SEI layer constructed via this concentration regulation, the HC anode delivered an initial capacity of 459.7 mAh g^{-1} at 0.1 C and retain 357.2 mAh g^{-1} after 500 cycles at 1 C. Diethylene glycol dimethyl ether (DEGDME) with 0.5 M $NaPF_6$ was evaluated in NIBs using polymer cathode. A reversible capacity of 206.7 mAh g^{-1} at 50 mA g^{-1}, a lifespan of 1500 cycles, and fast-charging capability up to 10 A g^{-1} were all demonstrated by the cells at room temperature [35]. This low-concentration electrolyte (0.5 M $NaPF_6$ in DEGDME) was also used for NIBs at −30 °C. Owing to the formation of an organic-rich cathode/electrolyte interphase, $Na_{0.7}Li_{0.03}Mg_{0.03}Ni_{0.27}Mn_{0.6}Ti_{0.07}O_2$//Na cells achieved a reversible capacities of 91.5 mAh g^{-1} and a capacity retention of 90.8% after 900 cycles at 1 C. In contrast, cells using PC-based electrolyte only retained capacities below 50 mAh g^{-1}, with rapid capacity decay until failure [36]. To optimize the low-temperature performance of Na/Na symmetric cells, different concentrations of THF blended with DEGDME were investigated. It was found that when adding 0.3 M $NaPF_6$ was introduced, fixing the DEGDME/THF volume ratio at 7:3 restricted the

Table 2
Comparison of various salts in sodium-based batteries.

Salt	Solvent system	Mole number	Ionic conductivity/ temperature	Ref.
$NaPF_6$	EC/DEC	0.2	3.7 mS cm^{-1}	[53]
$NaPF_6$	PC/FEC	0.3	4.24 mS cm^{-1}/25 °C	[26]
$NaPF_6$	PC/FEC/TTE	0.3	3.39 mS cm^{-1}/25 °C	[26]
$NaPF_6$	DEGDME	0.1	0.8 mS cm^{-1}	[54]
$NaPF_6$	DEGDME/DOL	0.4	3.62 mS cm^{-1}/−40 °C	[39]
$NaPF_6$	DEGDME	0.5	4.0 mS cm^{-1}/25 °C 1.7 mS cm^{-1}/−30 °C	[36]
$NaClO_4$	EC/PC	0.5	>6.5 mS cm^{-1}/25 °C	[25]
NaFSA	Succinonitrile (SN)	0.5	0.31 mS cm^{-1}/25 °C	[55]
NaBOB	TMP	0.5	5 mS cm^{-1}/22 °C	[31]
NaTDI	EC/DMC with 3%FEC		3.83 mS cm^{-1}/0 °C 6.29 mS cm^{-1}/20 °C	[52]
NaFSI	TEP/$PhCF_3$	0.16	3.5 mS cm^{-1}/30 °C	[56]
$NaSO_3CF_3$	1-methylimidazole	0.2	4.45 mS cm^{-1}	[51]

overpotential to merely 0.016 mV at a current density of 2.0 mA/cm^2 [37]. Additionally, a dual-salt electrolyte modified with TTE was developed using DEGDME as the base solvent. This electrolyte featured a weak Na^+ solvation shell and enabled a reversible capacity of 230.0 mAh g^{-1} in SMBs at −40 °C [38]. Yu's group [39] used 1,3-dioxolane (DOL) as a diluents to shield the Coulombic interaction between Na^+ and PF_6^-, as well as weaken the intermolecular forces of DEGDME, leading to improved Na^+-ion conductivity. The enhanced Na^+-PF_6^- interaction in the DOL-diluted electrolyte benefits the preferential anion decomposition during SEI formation. (Fig. 5(d)). DOL participated in the solvation sheath of Na^+, reducing the chelation strength between Na^+ and DEGDME to facilitate desolvation kinetics (Fig. 5(e)). Consequently, the low-concentration electrolyte (0.4 M $NaPF_6$ in DEGDME/DOL) achieved a Coulombic efficiency exceeding 99.9% at an ultralow temperature of −55 °C. For practical application validation, a 1 Ah capacity pouch cell of initial anode-free sodium metal battery retained 95% of its initial discharge capacity over 100 cycles at −25 °C (Fig. 5(f)).

Ether solvents enable enhanced cycling stability and rapid sodiation kinetics in electrode materials for SBBs. This benefit can be attributed to the favorable interplay between the electrolyte and electrode, including robust chemical compatibility and superior wettability. However, their specific chemical properties remain under investigation. Furthermore, these understudied properties continue to pose challenges for their practical application, such as limited compatibility with high-voltage cathodes and potential reactivity toward sodium metal anodes.

3. Salts and their concentrations

3.1. Salt classification

Anions primarily dictate the desolvation activation energy by tailoring the chemical properties of the salt as Na^+ ions migrate across the interphase layer [40]. Typically, anions with lower donor numbers, such as PF_6^- and ClO_4^-, require less desolvation energy (approximately 20 kJ mol^{-1}), whereas salts like sodium trifluoromethanesulfonate (NaOTf) around 80 kJ mol^{-1} [41]. Thus, in the design of high-performance low-concentration electrolyte chemistries, the optimization of both salt anions and solvents must be emphasized. Salts including $NaClO_4$, $NaPF_6$, NaBOB, NaFSI, NaTFSI and $NaCF_3SO_3$, similar to those used in lithium-ion batteries, are widely reported in low-concentration SSBs (Table 2). Among these, $NaPF_6$ has become a mainstream electrolyte salt for sodium batteries, as it shares a comparable synthesis pathway and compatibility with the production processes and equipment used for $LiPF_6$. Furthermore, studies on the passivation of aluminium current collectors have shown that a passivating $AlF_3/AlO_{x/2}F_{3-x}$ film forms when $NaPF_6$ is used, helping to prevent aluminium corrosion [42]. A 0.3 M $NaPF_6$ electrolyte in ester-based solvents for sodium ion batteries [20,26] and in ether-based solvents for sodium metal batteries [37] exhibits low viscosity and acceptable ionic conductivity. This property effectively reduces cell impedance and improves cell performance under low-temperature conditions. Owing to the overall performance of $NaPF_6$, ultra-low concentration (<0.3 M) have been investigated to reduce electrolyte cost [43]. Compared to $NaPF_6$, which exhibits extreme sensitivity to water and subsequent production of toxic HF, $NaClO_4$ was also widely used due to its suitable electrochemical window in carbonates, along with its lower cost and higher stability [44]. Deng et al. [22] found that $NaClO_4$ dissociates completely (Na^+ and ClO_4^- with no interaction) in a 0.3 M low-concentration electrolyte; however, its probable solvation structure requires additional energy to overcome the dissociation barrier. In contrast, Na^+ and ClO_4^- still interact in a 1.0 M standard electrolyte, and the self-constructed Na^+/solvent structure facilitates ion desolvation during charge transfer.

Xu and Angell [45] first synthesized and characterized lithium bis(oxalato)borate (LiBOB), and since then, this compound has been widely used in lithium-ion batteries with considerable success, functioning both as a standalone salt and an additive. However, NaBOB was first made by Zavalij et al. in 2003 and is considered insoluble in the organic solvents needed for practical applications [46]. Mogensen et al. [32] adopted TMP as nonflammable solvent, 0.5 M NaBOB was fully soluble in TMP and presents an ionic conductivity of 5 mS cm^{-1} at room temperature. Similarly, the low-toxicity and flame-retardant electrolyte of 0.38 M NaBOB in TEP delivered thousands of cycles of long-term performance at high temperatures. In low-concentration electrolyte, NaTFSI and NaFSI can cause the corrosion of aluminum current collectors when high-potential cathodes are used, leading to the formation of soluble $Al(TFSI)_3$ or $Al(FSI)_3$ [47]. To address this issue, anions such as $DFOB^-$ and PF_6^- have been used as Al corrosion inhibitor added to FSI^-- or $TFSI^-$-based electrolytes [48]. Additionally, low-concentration NaFSI (0.25 M) [49] and NaTFSI (0.5 M) [50] were studied in ionic liquids, which possess intrinsic ionic conductivity, wide electrochemical windows, superior thermal stability, non-flammability, and non-volatility.

0.2 M $NaCF_3SO_3$ dissolved in 1-methylimidazole (Melm) ensures high ionic conductivity and low cost, making it suitable for graphite anodes in SIBs. In this designed electrolyte, solvated Na^+ ions are initially intercalated but not released; instead, they support graphite layers to enhance rate performance by facilitating subsequent Na^+ intercalation/deintercalation, and interact with Melm to prevent graphite peeling and enhance cycle stability. As a result, the resulting C//Na half-cell demonstrates a long life of over 1800 cycles (with ~84.6% capacity retention), while the $NaTi_2(PO_4)_3$//C full cell achieves a lifespan exceeding 2800 cycles [51]. The low coordinating Hückel-type salt (4,5-dicyano-2-(trifluoromethyl)imidazolate, NaTDI) was studied in ether-based electrolyte. The optimal properties were observed for 0.75 M NaTDI in EC/DMC (1:1 v/v) with 3% FEC additive, which exhibited a conductivity of 11.52 mS cm^{-1} at room temperature [52]. When 0.25 M NaOTf and 0.25 M $NaPF_6$ are dissolved in DEGDME, they exhibit weak

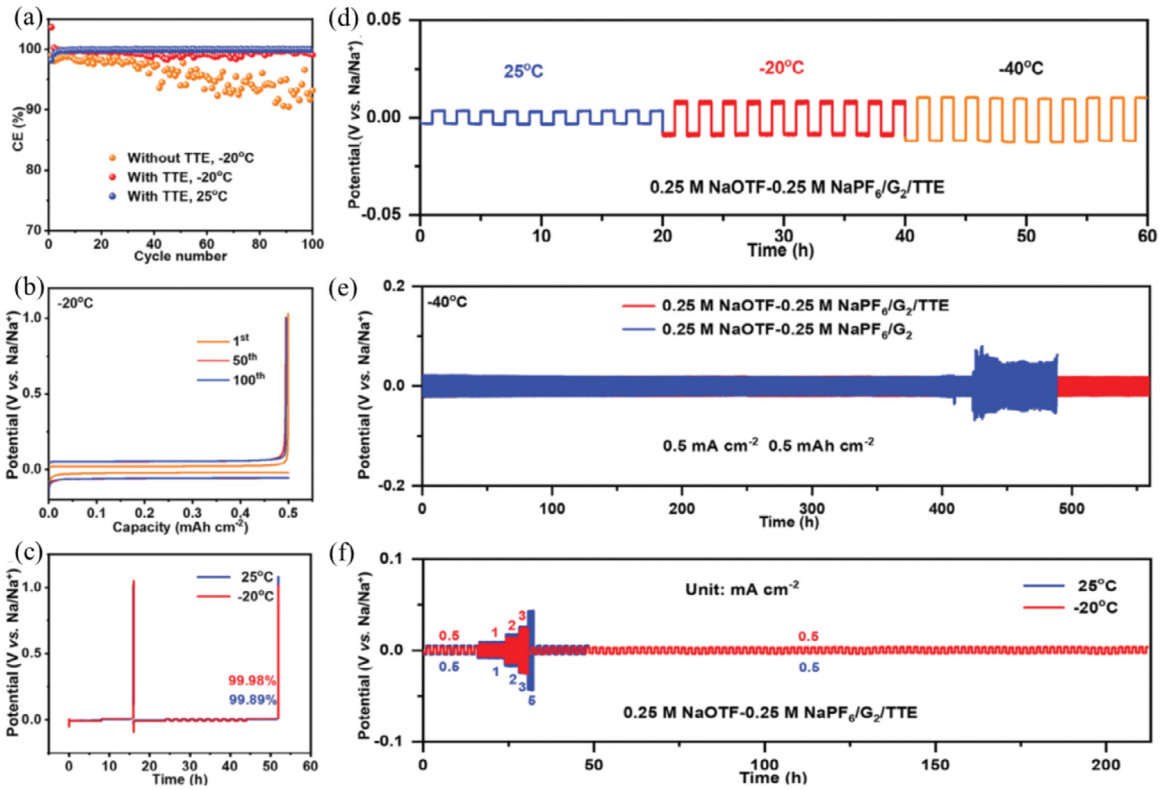

Fig. 6. (a) Coulombic efficiencies of Na//Al@C cells at different temperatures with the current density/plating capacity of 0.5 mA cm^{-2}/0.5 mAh cm^{-2} under 1.0 V charge cut-off potential, and (b) the representative potential capacity curves of Na//Al@C half cells at low temperature. (c) Average CE measurements of Na//Al@C half cells. (d) Galvanostatic profiles of Na//Na symmetrical cells from 25 to −40 °C (d) and at −40 °C (e) with the current density/plating capacity of 0.5 mA cm^{-2}/0.5 mAh cm^{-2}. (f) Galvanostatic profiles of Na//Na symmetrical cells at 25 °C and −40 °C at different current densities. Reproduced with permission [38]. Copyright 2024, Wiley-VCH.

solvation. This weak solvation promotes fast ion transport, enabling smooth Na plating, and also facilitates the formation of a NaF-rich SEI layer. The Na//Al@C half-cell based on the this LCE exhibits an average CE as high as 99.36% during 100 cycles at −20 °C (Fig. 6(a)), with an overpotential of 0.115 V after 100 cycles and a maintained average CE of 99.98% (Figs. 6(b)(c)). Na//Na symmetrical cells adopting this low-concentrated dual-salt electrolyte delivered stable potential profiles during different temperature and current ranges (Figs. 6(d)–(f)). Consequently, this SMB achieves a reversible capacity of 202.8 mAh g^{-1} at −20 °C and 1 C [38].

3.2. Concentration and solvation structure regulation

Low salt concentrations significantly influence solvation structures and electrochemical performance. Unlike high-concentration electrolytes, which are dominated by CIPs and AGGs, low-concentration systems favor SSIPs. In LCEs, Na^+ ions are typically solvated by polar solvents, and more solvent molecules participate in electrode interface reactions. This weakens cation-anion interactions but leads to the formation of unstable organic-enriched SEI/CEI. This weakly solvating environment reduces desolvation energy barriers, boosting ion transport kinetics and low-temperature performance [6,13]. However, LCEs face challenges inherent to their solvation structure, free solvent molecules decompose preferentially, forming organic-rich, fragile electrode/electrolyte interface that lack inorganic components (e.g., NaF) necessary for dendrite suppression in SBBs.

Shi et al. [57] designed a dual-weak-interaction electrolyte (DWIE) by manipulating dipole interactions among different solvent molecules. This electrolyte system employs weakly solvated tetrahydrofuran as the inner solvation shell and introduces dipole interactions in the outer layer using dibutyl ether, thereby further reducing the binding energy between cations and solvents and ultimately realizing an anion-engaged solvation structure. By selecting THF, a primary solvent with weak coordination to sodium ions, and introducing dipolar interactions between the co-solvent dibutyl ether (DBE) and THF, the binding energy between Na^+ and THF is further weakened. This promoted more FSI^- to coordinate with Na^+, achieving a solvation structure dominated by CIPs and AGGs at low salt concentrations. Benefiting from the anion-derived inorganic-rich SEI, the SBBs achieved a cycling lifespan of 217 cycles. Additionally, at 5 C rate, the NVP/Na battery demonstrated stable cycling for over 3000 cycles. Wang's group [58] presented a strategy for solvent-structured regulation in LCEs. As the salt concentration decreases to 0.4 M, the coordination number of Na^+ with PC increases to 4.67, whereas that of Na^+ with ClO_4^- decreases to 0.78 (Figs. 7(a)–(e)). This phenomenon can be attributed to the diminished ion-to-solvent ratio. On the contrary, in the 0.4PTF (0.4 M $NaClO_4$ in PC/TTE/FEC) electrolyte, the CN of Na^+–PC reduces to 4.00 while the CN of Na^+–ClO_4^- can be increased. According to the calculated coordination environment details, in the designed 0.4PTF electrolyte, the solvation structure showed the proportion of CIPs and AGGs increases significantly to 88.9% (Fig. 7(f)). Pan's group [56] proposed a solvent reorganization strategy for developing highly stable dilute phosphate electrolytes. Optimal intermolecular interactions between the main phosphate solvent and trifluorotoluene ($PhCF_3$) drive this solvent reorganization. By strengthening the solvation network, this $PhCF_3$-induced structure enables a highly stable dilute phosphate electrolyte, particularly when synergistic additives are incorporated. Using this designed LCEs, $NaCu_{1/9}Ni_{2/9}Fe_{1/3}Mn_{1/3}O_2$ (CNFM)/HC full cells achieve a lifespan of 400 cycles with >99.95% CE. An Ah-level pouch cell demonstrates safe cycling over 100 cycles at 60 °C, retaining 90.1% capacity without inflation.

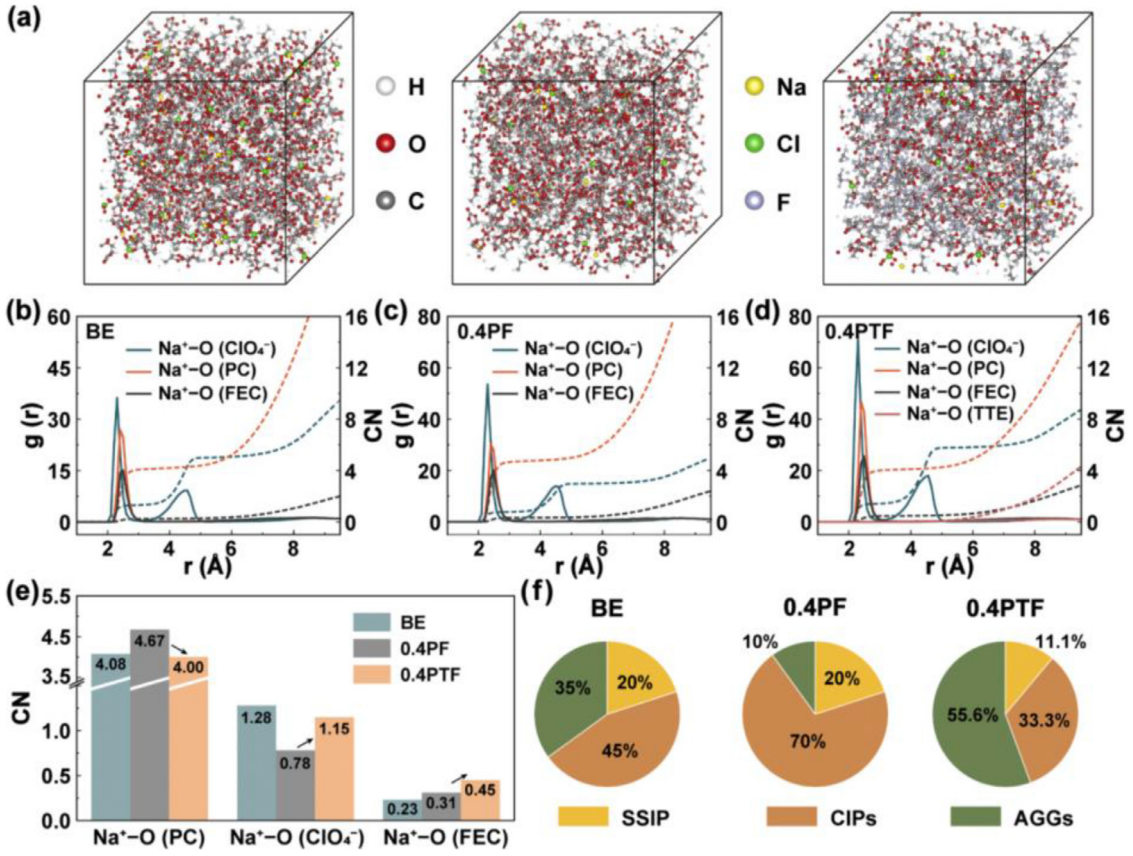

Fig. 7. (a) Snapshots of three electrolytes obtained from cMD simulations. (b)–(e) Radial distribution functions and coordination numbers of Na^+ in different electrolytes. (f) Population statistics of SSIPs, CIPs and AGGs in different electrolytes. Reproduced with permission [58]. Copyright 2025, Elsevier.

4. Additive design

4.1. Fluoroethylene carbonate

A viable strategy to enhance the anodic stability of conventional electrolytes involves incorporating fluorinated organic compounds, especially in low-concentration electrolyte. Thanks to their fluorine-containing groups, these compounds can undergo preferential reactions on both the anode and cathode when the electrodes are polarized, forming protective surface films prior to the decomposition of the base electrolyte components [59,60]. Among such additives, FEC is widely utilized for constructing NaF-rich SEI on anodes through preferential reduction [61]. Komaba et al. [62] compared different commonly used and effective film-forming additives for LIBs, including fluoroethylene carbonate (FEC), difluoroethylene carbonate (DFEC), and vinylene carbonate (VC), only FEC demonstrated effectiveness in SIBs. This observation underscores the necessity of dedicated research on electrolyte additives for SIBs, rather than direct extrapolation of findings from LIB studies. Xing's group further found that VC produces harmful species in SIBs due to differences in reduced-state electrostatic potentials with Na^+. Similarly, DFEC deteriorates SIB performance due to distinct reduction pathways, while FEC retains its effectiveness across both systems due to consistent reduced-state structures and electrostatic potentials [63].

3%FEC was demonstrated does not significantly alter ionic conductivity but stabilizes SEI film in low-concentration SIBs [52]. Aladinli et al. [53] utilized FEC as an electrolyte additive in PC, which mitigated the undesired effects of PC and enabled reversible cycling. The electrolyte of 0.5 M $NaPF_6$ dissolved in PC/FEC delivered 98%–99% coulombic efficiency in dual-ion batteries. Based on the low-concentration electrolyte of 0.3 M $NaClO_4$-EC/PC, Deng et al. [22] explores the performance optimization mechanism of adding 5% FEC. The incorporation of FEC facilitates the formation of a weak solvation structure. Ab initio molecular dynamics simulations reveal that Na^+/solvent exists as solvent-separated ion pairs in the electrolyte, with a low binding energy of −67.5 kcal/mol, accelerating the desolvation process. Temperature-dependent EIS was used to study the interfacial kinetics of $Na_3V_2(PO_4)_2F_3$ (Figs. 8(a)–(d)). Compared to normal-used electrolyte (1.0 M $NaClO_4$+5%FEC), the weakly-solvating electrolyte (0.3 M $NaClO_4$ + 5%FEC) has lower charge transfer activation energy. Endowed with this weak solvation ability, the electrolyte facilitates the Na^+ desolvation process by reducing the energy barrier and promotes rapid charge transfer kinetics (Figs. 8(e)(f)). TOF-SIMS and XPS characterizations further confirmed that FEC induces the formation of a dense and uniform CEI, which is rich in Na_2CO_3 and low in NaF, reducing Na^+ transport resistance. Consequently, the $Na_3V_2(PO_4)_2F_3$ cathode achieved 93.4% retention after 1000 cycles at −25 °C; additionally, the NVPF/HC full cell operates stably for over 300 h. FEC synergistically improves low-temperature kinetics and cycling stability by regulating interfacial chemistry and solvation structure.

4.2. Other fluorinated additives

Similar to lithium-ion batteries, in sodium-ion battery electrolyte systems, unsaturated carbonates, compounds containing fluorine, sulfur, silicon, phosphorus, as well as inorganic sodium salts are commonly reported to improve the electrode/electrolyte interface [16,64,65]. These additives possess high reactivity and can be preferentially oxidized/reduced in the electrolyte, inhibiting the decomposition of other electrolyte components. Consequently, they enhance the high and low-temperature performance, rate capability of sodium-ion batteries, and suppress gas generation and swelling [66]. Currently, in

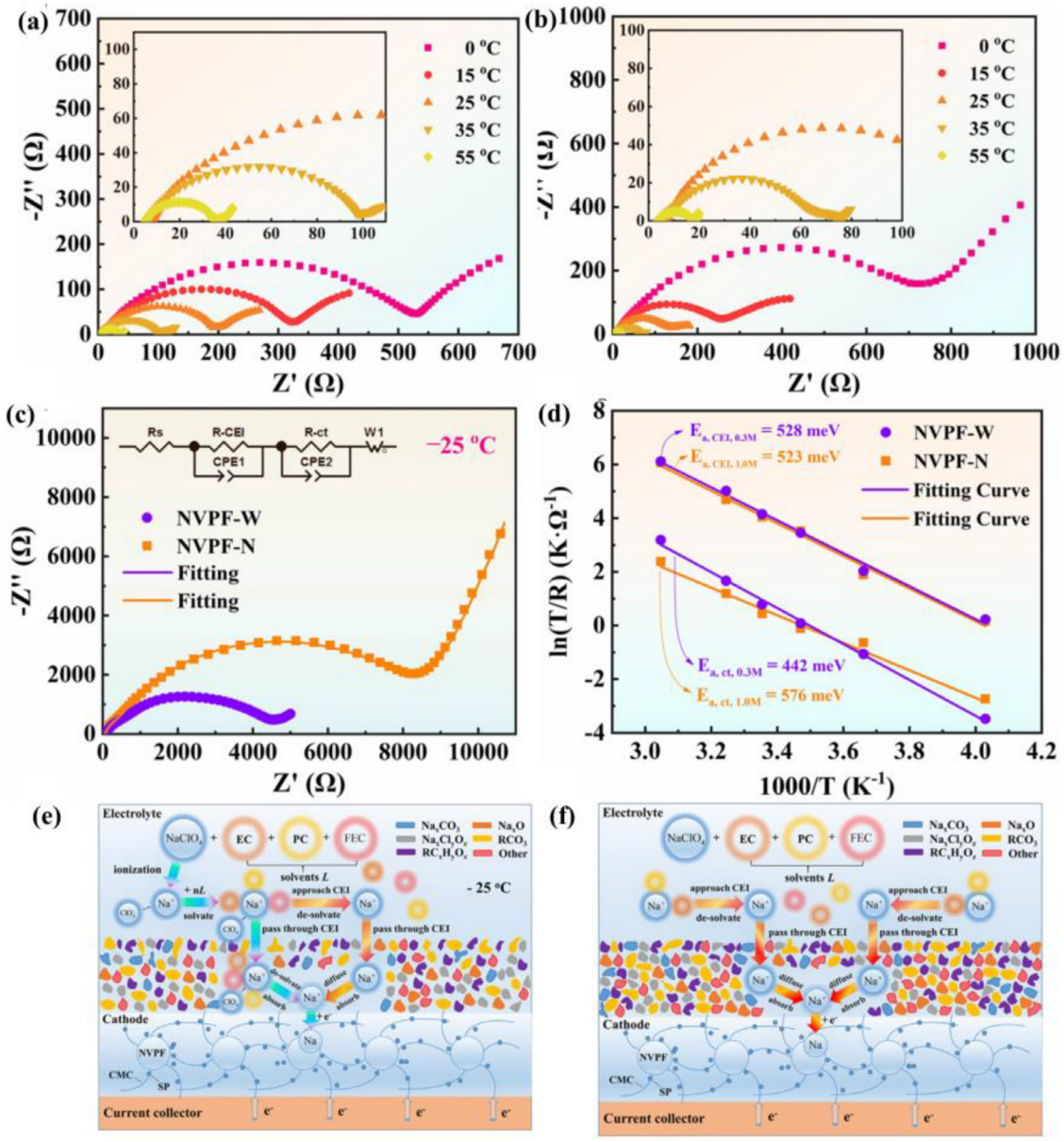

Fig. 8. Interfacial kinetics at the cathode/electrolyte interface probed by temperature-dependent EIS. Nyquist plots of the NVPF-W cathode (a) and NVPF-N cathode (b). (c) Comparison of the Nyquist plots at low temperature; (d) Arrhenius plots for charge transfer resistance (R_{ct}) and CEI (R_{CEI}) in various electrolytes. Schematic of the NVPF/interface/electrolyte system in the standard (e) and weakly-solvating (f) electrolytes. Reproduced with permission [28]. Copyright 2022, Elsevier.

low-concentration electrolyte systems, besides FEC, other fluorine-containing additives have also attracted significant attention.

N, O-bis(trimethylsilyl) trifluoroacetamide (BSTFA) was incorporated into a low-concentration electrolyte (0.3 M $NaPF_6$ in EC/PC, 1:1 v/v) to stabilize the electrolyte matrix and construct a highly conductive electrode/electrolyte interface for SMBs. Theoretical simulations combined with experimental characterizations confirm that BSTFA exhibits spontaneous scavenging activity toward HF and H_2O impurities in the $NaPF_6$-based electrolyte, thereby suppressing the hydrolysis of $NaPF_6$. Benefiting from the formation of protective SEI and CEI, $Na||Na_3V_2(PO_4)_3$ cells employing the electrolyte with 2% BSTFA achieve a capacity retention of 92.63% after 1955 cycles at 2 C, alongside a high-rate capability of over 105 mAh g^{-1} at 40 C [21]. The dual additives of sodium difluoro(oxalato)borate (NaDFOB) and tris(trimethylsilyl)borate (TMSB) in low-concentration electrolyte (0.3 M $NaPF_6$ in EC/PC, 1:1 v/v) were also demonstrated to improve the cycling performance of the hard carbon/$NaNi_{1/3}Fe_{1/3}Mn_{1/3}O_2$ cell by constructing interface films on the anode and cathode. By incorporating dual additives, the capacity retention increased from 17% to 83% after 200 cycles at room temperature [67]. 1 wt% 2,2,2-trifluoroethyl acetate (ETFA) was added into a low-concentration electrolyte (0.5 mol L^{-1} $NaPF_6$-PC/EMC). By decreasing viscosity, increasing ionic conductivity, and altering the solvation structure at low temperatures, the ETFA additive enabled superior performance. Specifically, the cell retained 92.1% of its initial capacity after 1120 cycles at 1 C and −20 °C [23]. In the high-voltage sodium-ion battery system with ultra-low concentration (≤ 0.3 M) ether-based electrolytes, the decrease in salt concentration promotes the full dissociation of sodium salts in solvents, leading the electrode-electrolyte interface to be predominantly composed of organic components derived from solvent decomposition. To address this issue, 0.03 M $NaBF_4$ was introduced as an additive into the 0.27 M $NaPF_6$-G2 electrolyte. This additive exerts little influence on the ionic conductivity of the pristine electrolyte (Fig. 9(a)) and the electrolyte can withstand voltages above 4.6 V (Fig. 9(b)). $NaBF_4$ effectively weakens

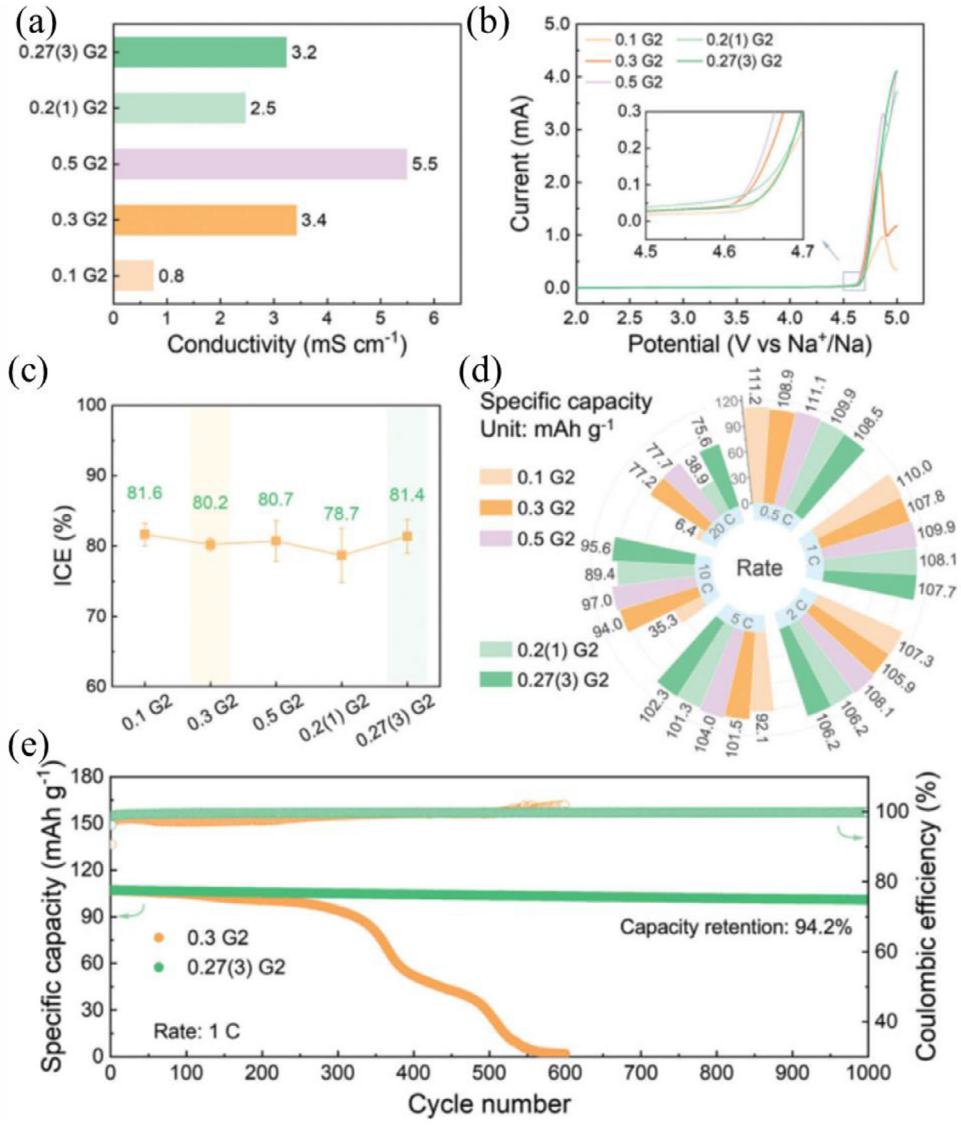

Fig. 9. Physicochemical and electrochemical characterization of the designed electrolytes. (a) Ionic conductivity and (b) LSV curves of different electrolytes. (c) ICE values for Na//NVOPF cells with distinct electrolytes. (d) Rate capabilities of Na//NVOPF cells employing various electrolytes. (e) Cycling stability of Na//NVOPF cells with various electrolytes at 1 C. Reproduced with permission [54]. Copyright 2025, Wiley-VCH.

the coordination between Na^+ and G2 molecules and prompting more PF_6^- to enter the solvation sheath of Na^+, thereby significantly enhancing cycling stability without sacrificing the high-rate performance (up to 20 C) of the $Na_3(VOPO_4)_2F$ cathode (Figs. 9(c)(d)). The designed electrolyte regulated by $NaBF_4$ enables the cells to achieve a capacity retention of 94.2% after 1000 cycles at 1 C (Fig. 9(e)) [54].

In the future application of these additives, efforts should focus on exploring their decomposition mechanisms and attempting to use multiple additives synergistically to enhance the overall performance of batteries. Meanwhile, impurities present in some additive components can have a significant negative impact on battery performance. Therefore, subsequent research on additives should also prioritize reagent purity. For additive manufacturers, optimizing production processes, reducing costs, and ensuring high product purity remain major challenges.

5. Conclusions and perspectives

Low-concentration electrolytes (LCEs) exhibit advantages in cost reduction, improved wettability, low viscosity, and enhanced low-temperature performance for SBBs. Unlike HCEs and LHCEs, which rely heavily on high salt content to form anion-rich solvation structures and inorganic-rich interphases. LCEs offer a more economically viable pathway for large-scale energy storage applications. However, their practical implementation is still hindered by challenges such as insufficient ionic conductivity, unstable electrode-electrolyte interfaces, and poor cycling stability, particularly at high voltages and extreme temperatures.

Key strategies for optimizing LCEs are primarily driven by solvation structure regulation and interfacial chemistry optimization. Solvent engineering, encompassing carbonate (e.g., PC, EC, EMC) and non-carbonate (e.g., DME, DEGDME, TMP), modulates dipole interactions and solvation strength. Weakly solvating co-solvents (e.g., TTE, DOL) reduce cation-solvent binding energy, enabling anion participation in solvation shells. Additives such as FEC, BSTFA, and $NaBF_4$ play critical roles in forming stable, ion-conductive SEI/CEI layers, scavenging harmful impurities, and enhancing desolvation kinetics. Salt selection ($NaPF_6$, $NaClO_4$) and concentration tuning shift solvation structures from SSIPs toward CIPs and AGGs, balancing ion transport kinetics and interfacial stability. Consequently, these strategies effectively improve the electrochemical performance of LCEs. The electrolyte of 0.3 M $NaClO_4$ in EC/PC with 5%FEC achieves 93.4% capacity reten-

tion after 1000 cycles at −25 °C; 0.2 M $NaCF_3SO_3$ in imidazole-based electrolyte delivers a capacity retention of 84.6% over 1800 cycles; and trace amounts of $NaBF_4$ modulates solvation sheaths to enable 94.2% retention at 1 C for 1000 cycles.

However, several critical challenges persist for LCEs in SBBs. The fundamental understanding of solvation structure and interfacial evolution in LCEs is still incomplete. The formation of organic-dominated interphases in LCEs often leads to poor mechanical stability and continuous electrolyte decomposition. Furthermore, the compatibility of LCEs with high-voltage cathodes and sodium metal anodes requires further improvement to prevent dendritic growth and cathode degradation. Future perspectives on the holistic design and component optimization of electrolytes are summarized as follows:

(1) Multi-component electrolyte systems that integrate non-solvating diluents, functional additives, and advanced salts to achieve synergistic effects can be developed to address the electrode/electrolyte interface instability. Such systems should enable anion-dominated solvation even at low concentrations, facilitating the formation of robust, inorganic-rich interphases.
(2) Electrolytes should be customized for specific operating conditions, such as high voltage, wide temperature range, or fast charging, by optimizing solvent polarity, salt dissociation ability, and additive composition. For example, ether-based LCEs show great promise for low-temperature applications, while phosphate-based systems offer improved safety.
(3) Complementary strategies, such as efficient functional additives, artificial interphases, surface coatings on electrodes, can further stabilize interfaces in LCE-based cells. These approaches can mitigate the limitations of LCEs and enhance overall battery performance.
(4) High-voltage compatibility (> 4.5 V) requires further optimization. Fluorinated co-solvents (PFPN) extend oxidation stability but raise toxicity concerns. Developing fluorine-free alternatives (e.g., phosphazene derivatives) with tailored HOMO-LUMO levels could balance stability and sustainability. Scaling up the synthesis of high-purity, low-cost additives will be crucial for commercial adoption.
(5) Excessive free solvents persist, forming soluble organic-rich interfaces. Future research should integrate molecular dynamics simulations and in situ characterization (cryo-TEM, TOF-SIMS) to decode how inter-solvent interactions (e.g., dipole-dipole effects in THF/DBE) modulate SSIP-CIP equilibria, aiming to replicate anion-dominated solvation without high salt loads. These insights will guide the rational design of electrolytes with tailored properties.

In conclusion, LCEs represent a promising direction for developing low-cost, high-performance sodium-based batteries. While significant progress has been made in understanding and optimizing their chemistry. Interdisciplinary efforts combining materials science, electrochemistry, and engineering are needed to overcome existing barriers. With continued innovation, LCEs are expected to play a vital role in the future of sustainable and scalable energy storage.

Declaration of Competing Interest

The authors declare the following personal relationships which may be considered as competing interests: Kang Wang is currently employed by Guangzhou Great Power Energy & Technology Company Limited. Other authors declare that there are no competing interests.

CRediT authorship contribution statement

Kang Wang: Writing – original draft, Investigation, Conceptualization. **Yongyao Feng:** Methodology, Investigation. **Jiajun Wang:** Investigation. **Jiaxiang Zeng:** Software. **Yuxin Guo:** Software. **Jiayi Wang:** Investigation. **Fangyuan Deng:** Software. **Qi Peng:** Investigation. **Feng Liu:** Methodology. **Kuirong Deng:** Visualization, Supervision. **Kai Yang:** Visualization, Validation. **Yilong Lin:** Writing – review & editing, Investigation, Funding acquisition, Conceptualization.

Acknowledgements

The authors would like to acknowledge the support from the National Nature Science Foundation of China (Grant No. 52402291), Special Project in Key Areas for Ordinary Universities in Guangdong Province (2024ZDZX3075), Advanced Electronic Materials Innovation Team Project for Ordinary Universities in Guangdong Province (2024KCXTD061), Guangdong Provincial Science and Technology Innovation Strategy Special Fund Project (pdjh2024b692).

References

[1] H. Yang, D. Wang, Y.L. Liu, Y.H. Liu, B.H. Zhong, Y. Song, Q.Q. Kong, Z.G. Wu, X.D. Guo, Improvement of cycle life for layered oxide cathodes in sodium-ion batteries, Energy Environ. Sci. 17 (2024) 1756–1780, doi:10.1039/D3EE02934D.
[2] Y.J. Guo, R.X. Jin, M. Fan, W.P. Wang, S. Xin, L.J. Wan, Y.G. Guo, Sodium layered oxide cathodes: Properties, practicality and prospects, Chem. Soc. Rev. 53 (2024) 7828–7874, doi:10.1039/D4CS00415A.
[3] Z.Y. Cheng, F.H. Cui, Y.W. Yao, Y.C. Ke, D.X. Cao, J. Yan, C.Y. Zhu, K. Zhu, Design of soft/hard interfaces with stress variation for improved sodium ion storage, Adv. Funct. Mater. 35 (2025) 2424000, doi:10.1002/adfm.202424000.
[4] X. Li, T. Zhang, Y.L. Zhao, X.Q. Zhu, A.M. Ge, K.C. Gordon, F. Wang, G.Y. Xu, M.F. Zhu, Enhancing robustness and charge transfer kinetics of sodium-ion batteries through introduction of anionic anchoring separators, J. Am. Chem. Soc. 147 (2025) 8488–8499, doi:10.1021/jacs.4c16227.
[5] L. Liu, Z. Shadike, N. Wang, Y.M. Chen, X.Y. Cai, E.Y. Hu, J.L. Zhang, Low concentration electrolyte: A new approach for achieving high performance lithium batteries, eScience 4 (2024) 100268, doi:10.1016/j.esci.2024.100268.
[6] Z.Y. Song, Z.R. Xing, J.X. Yang, J.Y. Chen, W.C. Hu, P. Li, W.F. Feng, G.G. Eshetu, E. Figgemeier, S. Passerini, M. Armand, Z.B. Zhou, H. Zhang, Electrolyte chemistry development for sodium-based batteries: A blueprint from lithium or a step toward originality? Angew. Chem. Int. Ed. 64 (2025) e202424543, doi:10.1002/anie.202424543.
[7] J.M. Zheng, J.A. Lochala, A. Kwok, Z.Q.D. Deng, J. Xiao, Research progress towards understanding the unique interfaces between concentrated electrolytes and electrodes for energy storage applications, Adv. Sci. 4 (2017) 1700032, doi:10.1002/advs.201700032.
[8] M.H. Li, Y. Liu, X.M. Yang, Q. Zhang, Y.F. Cheng, L. Deng, Q.W. Zhou, T. Cheng, M.D. Gu, Acetonitrile-based local high-concentration electrolytes for advanced lithium metal batteries, Adv. Mater. 36 (2024) 2404271, doi:10.1002/adma.202404271.
[9] G.Z. Zhang, J.W. Li, S.S. Chi, J. Wang, Q.R. Wang, R.H. Ke, Z.B. Liu, H. Wang, C.Y. Wang, J. Chang, Y.H. Deng, J. Lu, Molecular design of competitive solvation electrolytes for practical high-energy and long-cycling lithium-metal batteries, Adv. Funct. Mater. 34 (2024) 2312413, doi:10.1002/adfm.202312413.
[10] Z.J. Wang, X.L. Guo, Y.Y. Dong, W.J. Qu, K. Wang, L.W. Dong, C.H. Yang, Z.T. Lei, J.Y. Liang, Low-concentration electrolyte engineering for rechargeable batteries, Adv. Mater. 37 (2025) 2501215, doi:10.1002/adma.202501215.
[11] K.T. Keasler, M.E. Zick, E.E. Stacy, J. Kim, J.H. Lee, L. Aeindartehran, T. Runcevski, P.J. Milner, Handling fluorinated gases as solid reagents using metal-organic frameworks, Science 381 (2023) 1455–1461, doi:10.1126/science.adg8835.
[12] J.M. Zheng, S.R. Chen, W.G. Zhao, J.H. Song, M.H. Engelhard, J.G. Zhang, Extremely stable sodium metal batteries enabled by localized high-concentration electrolytes, ACS Energy Lett. 3 (2018) 315–321, doi:10.1021/acsenergylett.7b01213.
[13] Y.S. Hu, H.L. Pan, Solvation structures in electrolyte and the interfacial chemistry for Na-ion batteries, ACS Energy Lett. 7 (2022) 4501–4503, doi:10.1021/acsenergylett.2c02529.
[14] Y. Li, Y.X. Lu, P. Adelhelm, M.M. Titirici, Y.S. Hu, Intercalation chemistry of graphite: Alkali metal ions and beyond, Chem. Soc. Rev. 48 (2019) 4655–4687, doi:10.1039/C9CS00162J.
[15] A. Yao, S.M. Benson, W.C. Chueh, Critically assessing sodium-ion technology roadmaps and scenarios for techno-economic competitiveness against lithium-ion batteries, Nat. Energy 10 (2025) 404–416, doi:10.1038/s41560-024-01701-9.
[16] X.Y. Zheng, L.Q. Huang, X.L. Ye, J.X. Zhang, F.Y. Min, W. Luo, Y.H. Huang, Critical effects of electrolyte recipes for Li and Na metal batteries, Chem 7 (2021) 2312–2346, doi:10.1016/j.chempr.2021.02.025.
[17] H.X. Liu, X.Y. Zheng, Y.M. Du, M.C. Borras, K. Wu, K. Konstantinov, W.K. Pang, S.L. Chou, H.K. Liu, S.X. Dou, C. Wu, Multifunctional separator enables high-performance sodium metal batteries in carbonate-based electrolytes, Adv. Mater. 36 (2024) 2307645, doi:10.1002/adma.202307645.
[18] Y.S. Hu, Y.X. Lu, The mystery of electrolyte concentration: From superhigh to ultralow, ACS Energy Lett. 5 (2020) 3633–3636, doi:10.1021/acsenergylett.0c02234.
[19] W.J. Zhang, Y.L. Zhang, J.K. Zhou, X.N. Li, W.Z. Zhou, D. Zhang, J. Mao, K.H. Dai, Optimizing electrochemical performance in sodium-ion batteries using O3-type $Na_{0.90}Cu_{0.22}Fe_{0.30}Mn_{0.48}O_2$ and hard carbon, J. Electrochem. Soc. 170 (2023) 070518, doi:10.1149/1945-7111/ace5e5.
[20] Y.Q. Li, Y. Yang, Y.X. Lu, Q. Zhou, X.G. Qi, Q.S. Meng, X.H. Rong, L.Q. Chen, Y.S. Hu, Ultralow-concentration electrolyte for Na-ion batteries, ACS Energy Lett. 5 (2020) 1156–1158, doi:10.1021/acsenergylett.0c00337.

[21] R. Jiang, L. Hong, Y.C. Liu, Y.D. Wang, S. Patel, X.Y. Feng, H.F. Xiang, An acetamide additive stabilizing ultra-low concentration electrolyte for long-cycling and high-rate sodium metal battery, Energy Storage Mater. 42 (2021) 370–379, doi:10.1016/j.ensm.2021.07.047.
[22] L. Deng, K. Goh, F.D. Yu, Y. Xia, Y.S. Jiang, W. Ke, Y. Han, L.F. Que, J. Zhou, Z.B. Wang, Self-optimizing weak solvation effects achieving faster low-temperature charge transfer kinetics for high-voltage $Na_3V_2(PO_4)_2F_3$ cathode, Energy Storage Mater. 44 (2022) 82–92, doi:10.1016/j.ensm.2021.10.012.
[23] X.M. Zhang, Z. Xu, J. Xie, Y.H. Lu, S.Y. Liu, X.W. Xu, J. Tu, B. Xu, X.B. Zhao, Nanoarchitectonics for a long-life and robust Na-ion battery at low temperature with prussian blue cathode and low-concentration electrolyte, J. Energy Storage 80 (2024) 110263, doi:10.1016/j.est.2023.110263.
[24] F. Huang, Y.P. Zhong, M.L. Qin, J.L. Qiu, C. Hu, P. Xu, H.Q. Zhang, C.Y. Sheng, S.Q. Liang, G.Z. Fang, Weakly anion-driven solvation towards stable operation of carbonate ester-based sodium metal batteries at -40 °C, Chem. Eng. J. 511 (2025) 162150, doi:10.1016/j.cej.2025.162150.
[25] Y. Lee, J. Lee, H. Kim, K. Kang, N.-S. Choi, Highly stable linear carbonate-containing electrolytes with fluoroethylene carbonate for high-performance cathodes in sodium-ion batteries, J. Power Sources 320 (2016) 49–58, doi:10.1016/j.jpowsour.2016.04.070.
[26] J.Y. Zeng, D.C. Guan, W.G. Wang, X. Tan, Y.B. Cao, Z.D. Peng, G.R. Hu, K. Du, Low-concentration electrolyte enables high-voltage positive electrode $Na_4Co_3(PO_4)_2P_2O_7$ with good cycle stability, ACS Appl. Energy Mater. 6 (2023) 4238–4248, doi:10.1021/acsaem.3c00120.
[27] Q.P. Zhang, X. Wang, H. Li, R. Qiao, Low-concentration electrolyte design for wide-temperature operation in sodium metal batteries, J. Electrochem. Soc. 172 (2025) 010501, doi:10.1149/1945-7111/ada372.
[28] Q. Li, G. Liu, H.R. Cheng, Q.J. Sun, J.L. Zhang, J. Ming, Low-temperature electrolyte design for lithium-ion batteries: Prospect and challenges, Chem. Eur. J. 27 (2021) 15842–15865, doi:10.1002/chem.202101407.
[29] Y. Li, F. Wu, Y. Li, M.Q. Liu, X. Feng, Y. Bai, C. Wu, Ether-based electrolytes for sodium ion batteries, Chem. Soc. Rev. 51 (2022) 4484–4536, doi:10.1039/D1CS00948F.
[30] K.R. Deng, Q.G. Zeng, D. Wang, Z. Liu, G.X. Wang, Z.P. Qiu, Y.F. Zhang, M. Xiao, Y.Z. Meng, Nonflammable organic electrolytes for high-safety lithium-ion batteries, Energy Storage Mater. 32 (2020) 425–447, doi:10.1016/j.ensm.2020.07.018.
[31] R. Mogensen, S. Colbin, A.S. Menon, E. Bjorklund, R. Younesi, Sodium bis(oxalato)borate in trimethyl phosphate: A fire-extinguishing, fluorine-free, and low-cost electrolyte for full-cell sodium-ion batteries, ACS Appl. Energy Mater. 3 (2020) 4974–4982, doi:10.1021/acsaem.0c00522.
[32] L.O.S. Colbin, R. Mogensen, A. Buckel, Y.L. Wang, A.J. Naylor, J. Kullgren, R. Younesi, A halogen-free and flame-retardant sodium electrolyte compatible with hard carbon anodes, Adv. Mater. Interfaces 8 (2021) 2101135, doi:10.1002/admi.202101135.
[33] X.Y. Wang, C. Yang, L.B. Yao, Y.C. Wang, N. Jiang, Y. Liu, Anion/cation solvation engineering for a ternary low-concentration electrolyte toward high-voltage and long-life sodium-ion batteries, Adv. Funct. Mater. 34 (2024) 2315007, doi:10.1002/adfm.202315007.
[34] F.H. Zeng, L.D. Xing, W.G. Zhang, Z.Y.T. Xie, M.Z. Liu, X.Y. Lin, G.X. Tang, C.Y. Mo, W.S. Li, Innovative discontinuous-SEI constructed in ether-based electrolyte to maximize the capacity of hard carbon anode, J. Energy Chem. 79 (2023) 459–467, doi:10.1016/j.jechem.2022.12.044.
[35] E.Y. Kim, M. Mohammadiroudbari, F. Chen, Z.Z. Yang, C. Luo, A carbonyl and azo-based polymer cathode for low-temperature Na-ion batteries, ACS Nano 18 (2024) 4159–4169, doi:10.1021/acsnano.3c08860.
[36] Y.H. Feng, M.T. Liu, J.X. Wu, C. Yang, Q. Liu, Y.W. Tang, X. Zhu, G.X. Wei, H.J. Dong, X.Y. Fan, S.F. Chen, W.Y. Hao, L.Z. Yu, X. Ji, Y. You, P.F. Wang, J. Lu, Monolithic interphase enables fast kinetics for high-performance sodium-ion batteries at subzero temperature, Angew. Chem. Int. Ed. 63 (2024) e202403585, doi:10.1002/ange.202403585.
[37] Z.Q. Wang, X.Y. Zheng, X.Y. Liu, Y.Y. Huang, L.Q. Huang, Y.W. Chen, M. Han, W. Luo, Promoting fast Na ion transport at low temperatures for sodium metal batteries, ACS Appl. Mater. Interfaces 14 (2022) 40985–40991, doi:10.1021/acsami.2c10915.
[38] D.D. Yu, Z.Y. Wang, J.C. Yang, Y.Y. Wang, Y.T. Li, Q.N. Zhu, X.M. Tu, D.Z. Chen, J.F. Liang, U. Khalilov, H. Wang, Low-temperature and fast-charge sodium metal batteries, Small 20 (2024) 2311810, doi:10.1002/smll.202311810.
[39] L. Hu, J.J. Deng, Y.X. Lin, Q.H. Liang, B.C. Ge, Q.S. Weng, Y. Bai, Y.S. Li, Y.H. Deng, G.H. Chen, X.L. Yu, Restructuring electrolyte solvation by a versatile diluent toward beyond 99.9% coulombic efficiency of sodium plating/stripping at ultralow temperatures, Adv. Mater. 36 (2024) 2312161, doi:10.1002/adma.202312161.
[40] K.L. Browning, R.L. Sacci, G.M. Veith, Energetics of Na^+ transport through the electrode/cathode interface in single solvent electrolytes, J. Electrochem. Soc. 164 (2017) A580–A586, doi:10.1149/2.0311704jes.
[41] E.H. Wang, Y.B. Niu, Y.X. Yin, Y.G. Guo, Manipulating electrode/electrolyte interphases of sodium-ion batteries: strategies and perspectives, ACS Mater. Lett. 3 (2021) 18–41, doi:10.1021/acsmaterialslett.0c00356.
[42] A. Konarov, H.J. Kim, H. Yashiro, S.T. Myung, Passivation of aluminum current collectors in non-aqueous carbonate solutions containing sodium or potassium hexafluorophosphate salts, J. Mater. Chem. A 7 (2019) 13012–13018, doi:10.1039/C9TA03911B.
[43] D.M.C. Ould, S. Oswald, H.E. Smith, C.A. O'Keefe, T.F. Song, E. Kendrick, D.S. Wright, C.P. Grey, Properties of $NaPF_6$ electrolytes and effect of electrolyte concentration on performance in sodium-ion batteries, Chem. Commun. 61 (2025) 8516–8519, doi:10.1039/D5CC01447F.
[44] F.Y. Cheng, M.L. Cao, Q. Li, C. Fang, J.T. Han, Y.H. Huang, Electrolyte salts for sodium-ion batteries: $NaPF_6$ or $NaClO_4$? ACS Nano 17 (2023) 18608–18615, doi:10.1021/acsnano.3c07474.
[45] W. Xu, C.A. Angell, LiBOB and its derivatives-weakly coordinating anions, and the exceptional conductivity of their nonaqueous solutions, Electrochem. Solid-State Lett. 4 (2001) E1–E4.
[46] P.Y. Zavalij, S.F. Yang, M.S. Whittingham, Structures of potassium, sodium and lithium bis(oxalato)borate salts from powder diffraction data, Acta Crystallogr. B 59 (2003) 753–759, doi:10.1107/S0108768103022602.
[47] G.C. Yan, X.H. Li, Z.X. Wang, H.J. Guo, W.J. Peng, Q.Y. Hu, Lithium difluoro(oxalato)borate as an additive to suppress the aluminum corrosion in lithium bis(fluorosulfony)imide-based nonaqueous carbonate electrolyte, J. Solid State Electrochem. 20 (2016) 507–516, doi:10.1007/s10008-015-3069-3.
[48] K. Park, S. Yu, C. Lee, H. Lee, Comparative study on lithium borates as corrosion inhibitors of aluminum current collector in. lithium bis(fluorosulfonyl)imide electrolytes, J. Power Sources 296 (2015) 197–203, doi:10.1016/j.jpowsour.2015.07.052.
[49] K. Biernacka, J. Sun, F. Makhlooghiazad, A. Balkis, I.E. Gunathilaka, L.A. O'Dell, M.G. Mestres, P.C. Howlett, J.M. Pringle, M. Forsyth, Electrochemical characterization of hexamethylguanidinium bis(fluorosulfonyl)imide HMG FSI based electrolyte and its application in sodium metal batteries, J. Phys. Energy 5 (2023) 014006, doi:10.1088/2515-7655/aca4a2.
[50] N. Wongittharom, T.C. Lee, C.H. Wang, Y.C. Wang, J.K. Chang, Electrochemical performance of $Na/NaFePO_4$ sodium-ion batteries with ionic liquid electrolytes, J. Mater. Chem. A 2 (2014) 5655–5661, doi:10.1039/C3TA15273A.
[51] W. Zhao, C.T. Wang, Z.J. Cheng, C. Zheng, Q. Yao, J. Pan, X.J. Ma, J. Yang, Revealing the Na storage behavior of graphite anodes in low-concentration imidazole-based electrolytes, Chem. Sci. 15 (2024) 6500–6506, doi:10.1039/D3SC06640A.
[52] A. Szczesna-Chrzan, T. Trzeciak, M. Zybert, H. Ronduda, A. Ostrowski, M. Trzaskowski, M. Drozd, M. Smolinski, G.Z. Zukowska, W. Raróg-Pilecka, W. Wieczorek, A. Buckel, R. Younesi, M. Marcinek, Systematic studies on liquid sodium 4,5-dicyano-2-(trifluoromethyl)imidazolate (NaTDI)-based electrolytes and its impact on the cycling behaviour against wet impregnated WI-NaNMC and prussian white cathodes, Adv. Mater. Interfaces 9 (2022) 2102012, doi:10.1002/admi.202102012.
[53] S. Aladinli, F. Bordet, K. Ahlbrecht, J. Tübke, M. Holzapfel, Anion intercalation into a graphite cathode from various sodium-based electrolyte mixtures for dual-ion battery applications, Electrochim. Acta 231 (2017) 468–478, doi:10.1016/j.electacta.2017.02.041.
[54] S.Q. Li, X.R. Song, P.W. Jing, X.Y. Xiao, Y.C. Chen, Q. Sun, M.X. Huang, Y.P. Zhang, G.S. Li, P.Y. Liu, S. Xu, Q.Y. Dou, J. Zhu, X.B. Yan, Trace $NaBF_4$ modulated ultralow-concentration ether electrolyte for durable high-voltage sodium-ion batteries, Adv. Funct. Mater. 35 (2025) 242249, doi:10.1002/adfm.202422491.
[55] K. Takada, Y. Yamada, E. Watanabe, J. Wang, K. Sodeyama, Y. Tateyama, K. Hirata, T. Kawase, A. Yamada, Unusual passivation ability of superconcentrated electrolytes toward hard carbon negative electrodes in sodium-ion batteries, ACS Appl. Mater. Interfaces 9 (2017) 33802–33809, doi:10.1021/acsami.7b08414.
[56] M.Y. Ma, B.B. Chen, X. Yang, Y.C. Liu, S. Dai, X.G. Qi, Y.S. Hu, H.L. Pan, Solvent reorganization and additives synergistically enable high-performance Na-ion batteries, ACS Energy Lett. 8 (2023) 477–485, doi:10.1021/acsenergylett.2c02353.
[57] T.Z. Shi, R.L. Hou, L.L. Zheng, H.Y. Lu, C.R. Xu, X.Y. Sun, P. He, S.K. Li, H.S. Zhou, S.H. Guo, Modulating double-layer solvation structure via dual-weak-interaction for stable sodium-metal batteries, Adv. Energy Mater. 15 (2025) 2405803, doi:10.1002/aenm.202405803.
[58] Y.H. Feng, Q. Liu, Y.H. Wang, S.F. Chen, S. Sun, Y.W. Tang, X. Zhu, G.X. Wei, T.L. Chen, M.T. Liu, X. Ji, H.S. Xin, P.F. Wang, Durable low-temperature sodium metal batteries enabled by solvent-interaction regulation in solvation structure, Energy Storage Mater. 81 (2025) 104453, doi:10.1016/j.ensm.2025.104453.
[59] Y.H.T. Tran, K.H. An, D.T.T. Vu, S.W. Song, High-voltage electrolyte and interface design for mid-nickel high-energy Li-ion batteries, ACS Energy Lett. 10 (2024) 356–370, doi:10.1021/acsenergylett.4c02860.
[60] S. Bolloju, N. Vangapally, Y. Elias, S. Luski, N.L. Wu, D. Aurbach, Electrolyte additives for Li-ion batteries: Classification by elements, Prog. Mater. Sci. 147 (2025) 101349, doi:10.1016/j.pmatsci.2024.101349.
[61] Z. Luo, L. Hu, C. Dai, G. Ma, Y. Ye, K. Xu, Z. Lin, Solvent chain-length engineering enables all-climate sodium-ion batteries, Angew. Chem. Int. Ed. 137 (2025) e202514451, doi:10.1002/ange.202514451.
[62] S. Komaba, T. Ishikawa, N. Yabuuchi, W. Murata, A. Ito, Y. Ohsawa, Fluorinated ethylene carbonate as electrolyte additive for rechargeable Na batteries, ACS Appl. Mater. Interfaces 3 (2011) 4165–4168, doi:10.1021/am200973k.
[63] Y.W. Li, D.P. Dong, J.H. Huang, F.H. Zeng, W.T. Liang, Z.Y.T. Xie, L.J. Quan, C. Chen, Y.H. Liao, D. Bedrov, L.D. Xing, W.S. Li, A miss is as good as a mile: Prediction of additive effectiveness in sodium-ion batteries based on electrostatic potential, ACS Energy Lett. 10 (2025) 2564–2573, doi:10.1021/acsenergylett.5c00039.
[64] Y.L. Lin, Q. Peng, L.W. Chen, Q. Zuo, Q.W. Long, F.H. Lu, S. Huang, Y.W. Chen, Y.Z. Meng, Organic liquid electrolytes in sodium-based batteries: Actualities and perspectives, Energy Storage Mater. 67 (2024) 103211, doi:10.1016/j.ensm.2024.103211.
[65] Y.X. Huang, L.Z. Zhao, L. Li, M. Xie, F. Wu, R.J. Chen, Electrolytes and electrolyte/electrode interfaces in sodium-ion batteries: From scientific research to practical application, Adv. Mater. 31 (2019) 1808393, doi:10.1002/adma.201808393.
[66] V. Shipitsyn, N. Antrasian, L.Q. Mu, L. Ma, Fundamentals and perspectives of electrolyte additives for non-aqueous Na-ion batteries, Energy Mater. 3 (2023) 300038, doi:10.20517/energymater.2023.22.
[67] Y.L. Lin, X.J. Jin, S.Q. Gao, F. Liu, S. Huang, X.R. Yang, Y.W. Chen, Y.Z. Meng, Improved interface construction on anode and cathode for Na-ion batteries using ultralow-concentration electrolyte containing dual-additives, Chem. Eur. J. 30 (2024) e202303741, doi:10.1002/chem.202303741.